Contents lists available at SCCE

Journal of Soft Computing in Civil Engineering

Journal homepage: www.jsoftcivil.com

Enhancing Structural Health Monitoring of Super-Tall Buildings Using Support Vector Machines, MEMD, and Wavelet Transform

Rouzbeh Doroudi [1]; Seyed Hossein Hosseini Lavassani [2,*]; Mohsen Shahrouzi [3]; Aref Afshar [4]

1. Ph.D., Faculty of Civil Engineering, Kharazmi University, Tehran, Iran
2. Associate Professor, Faculty of Civil Engineering, Kharazmi University, Tehran, Iran
3. Assistant Professor, Faculty of Civil Engineering, Kharazmi University, Tehran, Iran
4. Faculty of Civil Engineering, Kharazmi University, Tehran, Iran

* Corresponding author: *lavasani@khu.ac.ir*

https://doi.org/10.22115/scce.2024.429581.1763

ARTICLE INFO

Article history:
Received: 09 December 2023
Revised: 29 February 2024
Accepted: 18 March 2024

Keywords:
Structural health monitoring;
Multivariate empirical mode decomposition;
Super-tall buildings;
Wavelet transform;
Feature extraction;
Damage detection.

ABSTRACT

Super-tall skyscrapers are crucial for modern urbanization, but ensuring their safety in natural events is vital. Structural Health Monitoring (SHM) is essential for assessing the condition of these iconic structures. This study focuses on the Milad Tower in Tehran, Iran, and the Canton Tower in Guangzhou, China, aiming to detect, locate, and assess damage severity. The goal is to detect damage, locate affected areas, and assess severity. The following techniques are employed: a) Support Vector Machines (SVM), b) Multivariate Empirical Mode Decomposition (MEMD), c) Wavelet Transform (WT). SVMs efficiently identify damage patterns. However, require parameter tuning, addressed using Observer-Teacher-Learner-Based Optimization. MEMD interprets signals well, allowing simultaneous analysis of multiple signals, while WT eliminates noise from acceleration response data, enhancing damage detection accuracy. The investigation reveals that the optimized SVMs, combined with MEMD and WT, significantly improve sensitivity, accuracy, and effectiveness over conventional methods. With an accuracy of 99.60%, the proposed method outperforms other approaches, which have an accuracy of 96.02%, 92.32% and lower for those not utilizing WT and MEMD or optimizing the parameters of SVM, respectively. This demonstrates superior predictive capabilities. Additionally, the choice of appropriate features extracted from the time-series data plays a crucial role in enhancing damage detection and assessing structural health conditions. By integrating these techniques, engineers are enabled to process large-scale data effectively, detect damage promptly, and make informed decisions to support civil infrastructure management practices.

How to cite this article: Doroudi R, Hosseini Lavasani S H, Shahrouzi M, Afshar A. Enhancing structural health monitoring of super-tall buildings using support vector machines, memd, and wavelet transform. J Soft Comput Civ Eng 2025;9(1):91–121. https://doi.org/10.22115/scce.2024.429581.1763

2588-2872/ © 2025 The Authors. Published by Pouyan Press.
This is an open access article under the CC BY license (http://creativecommons.org/licenses/by/4.0/).

1. Introduction

The use of super-tall skyscrapers has become commonplace in recent years, thanks to impressive advancements in building materials, construction methods, and structural systems. These structures serve a variety of purposes, including lodging, hotels, communications, and business offices, thereby having an enormous impact on modern urbanization. The performance of these buildings is vital to structural engineering, especially concerning environmental stressors such as seismic activities and wind forces. Essentially, the major concern is determining whether these structures remain undamaged and safe during natural events. Structural Health Monitoring (SHM) refers to the method used to evaluate the condition of structures across various fields, such as civil, mechanical, and aeronautical engineering, to determine their structural integrity [1].

The primary objective of SHM is to continuously evaluate and interpret the diagnostic status of the constituent materials in different elements, as well as the overall collective of these components forming the entire structure, at all times throughout the structure's lifespan [2]. Hence, identifying damage is another important aspect of SHM. Features are required for damage detection, which are extracted by signal processing methods [3]. For SHM, features are derived through numerous signal processing methods, including algorithms that operate in both the time and frequency domains, which are grounded in the continuous domain [4].

Scholars have conducted numerous studies to recognize the safety and structural dynamics characteristics of high-rise buildings [5–14]. A range of signal processing methods including Short Time Fourier Transform (STFT), Fast Fourier transform (FFT), Empirical Mode Decomposition and Hilbert–Huang Transform (EMD-HHT) are utilized to assess dynamic characteristics of these structures. Despite the fact that these extremely tall buildings are appropriately outfitted with a variety of equipment to observe their structural dynamic states, in the majority of instances, the investigations only make use of a few sensors. Furthermore, nonlinear and nonstationary signals can pose challenges to certain signal processing techniques, including FFT and STFT.

Empirical Mode Decomposition (EMD) can effectively manage and solve nonlinear and nonstationary signals, distinguishing it from other time-frequency decomposition techniques. Consequently, many scholars have utilized EMD to assess structural conditions [15,16]. Despite the advantages listed, EMD can only be effective when signals are provided that have enough local extrema. It is also prone to mode mixing and is mainly intended for univariate data analysis [17]. To address these limitations, Multivariate Empirical Mode Decomposition (MEMD) is frequently utilized, particularly for analyzing multichannel signals [18]. This method can process all collected data from different sensors simultaneously, making MEMD a powerful tool for extracting the desired features for SHM.

SHM involves damage detection, where the aforementioned algorithms detect damage using extracted features. Vibration-based SHM detects damage through several structure-wide vibration signals. Damage detection may be done in the feature domain after extracting damage-sensitive features from the time series or in the time-domain using raw sensor data [19]. There

are two methods for structural status and damage detection. The first is physics-based, utilizing the natural frequency, mode, and curvature of structural systems to determine vibrational properties. The major challenge with this approach is the unclear physical models, such as complicated physical systems or insensitive physics-based characteristics [20]. Conversely, the data-driven approach is capable of extracting relevant features from sensor data for evaluating structural conditions [20]. Data-driven algorithms efficiently extract key information from complicated sensor data. The Auto-Regressive Moving Average with eXogenous (ARMAX) is one of the data driven models that is used to detect [21]. However, it has some limitations, such as being computationally expensive, less explainable than exponential smoothing, and vulnerable to non-stationary data (wind and acceleration response) as well as multivariate data (sensor data from complex SHM systems) [22]. Machine learning approaches, including Artificial Neutral Networks (ANN), Support Vector Machines (SVM) have drawn increasingly more attention to data mining for SHM applications among the data-driven approaches [23–26]. SVM algorithms are renowned for their efficiency in identifying damage and extracting features [27]. This approach provides great accuracy and sensitivity for damage identification [28]. Nonetheless, SVMs necessitate a substantial quantity of labeled examples and are vulnerable to challenges associated with data imbalance, being mainly suitable for binary classification tasks [29,30]. Also, the parameters of SVM need fine-tuning. Therefore, in this study, an optimization algorithm is used to fine-tune the parameters of SVM [31,32].

The SHM system employed in high-rise structures is intricate, capable of gathering diverse data types. Conversely, SHM systems on such super-tall buildings yield numerous collected signals. Therefore, MEMD proves invaluable for concurrently analyzing the complete signal to monitor the condition of these structures. MEMD excels in accurately identifying non-stationary and nonlinear vibration signals. Additionally, Wavelet Transform (WT) serves as a robust tool for eliminating noise that may arise during the operation of SHM systems with full-scale structures. Furthermore, SVM algorithms emerge as effective means for pattern recognition and damage identification. Consequently, integrating SVM with MEMD and WT proves beneficial for the detection of damage in full-scale structures, given the robust capabilities of these methods in feature extraction and pattern recognition within the realm of SHM.

The Milad Tower (Tehran, Iran) and the Canton Tower (Guangzhou, China), two real-world instances of very tall buildings, are investigated in this study. SVM are used to detect damage, location, and severity of damage. The model requires modification for several unknown variables, and optimization presents a systematic approach to address this. In recent decades, meta-heuristic algorithms have emerged as a prominently active field of study [33–35], aiming to transition from local optima to a global optimum. Given its previous success in various engineering tasks, Observer-Teacher-Learner-Based Optimization (OTLBO) is determined for this application [36,37]. One of the aims of this research is to evolve a technique to investigate all collected signals simultaneously to find out the damage detection of structures and select appropriate features. Consequently, MEMD is employed to determine the condition of the super-tall structures. Initially, both structures are subjected to wind load, then the acceleration responses of the structures are refined by WT to eliminate noise and identify proper frequencies.

Subsequently, the filtered signals are broken down through MEMD into different Intrinsic Mode Functions (IMFs), and finally, statistical parameters of IMFs are used as features for damage detection by the optimally tuned SVM. Figure 1 illustrates the schematic of the suggested model.

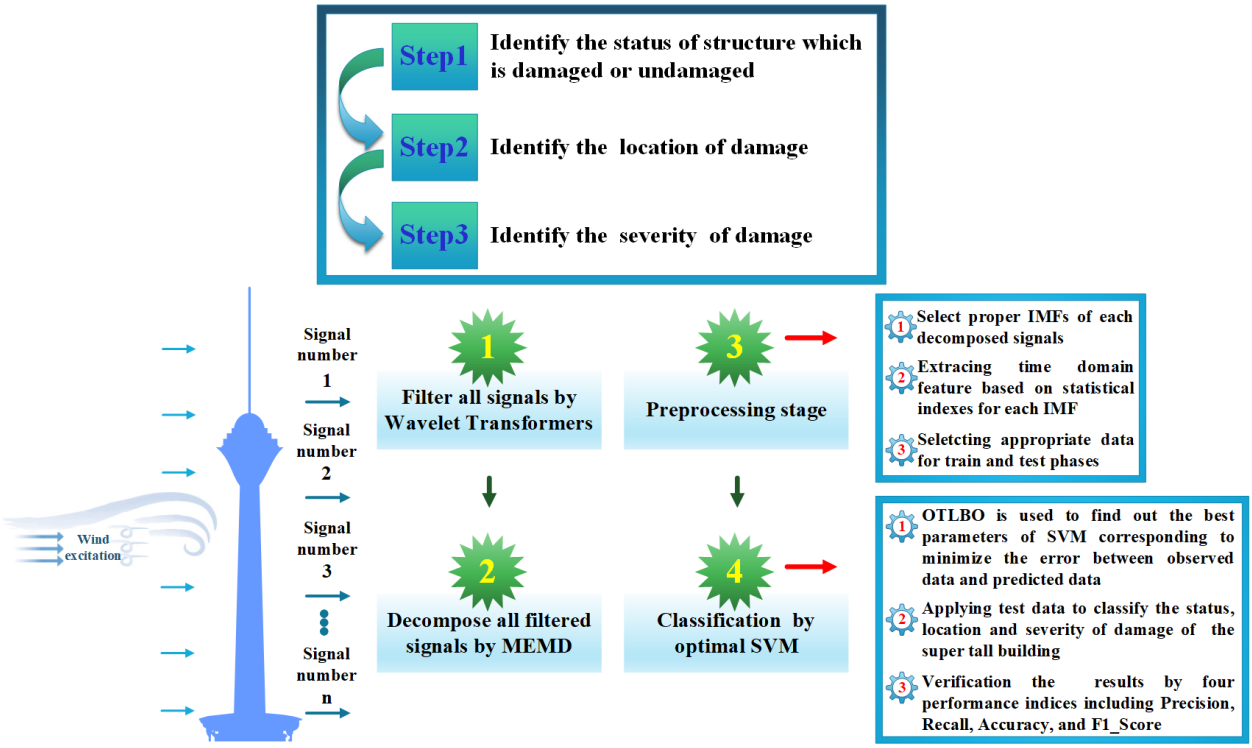
Step1
Identify the status of structure which is damaged or undamaged
Step2
Identify the location of damage
Step3
Identify the severity of damage
Wind excitation
Signal number 1
Signal number 2
Signal number 3
Signal number n
1
Filter all signals by Wavelet Transformers
2
Decompose all filtered signals by MEMD
3
Preprocessing stage
4
Classification by optimal SVM
Select proper IMFs of each decomposed signals
Extracing time domain feature based on statistical indexes for each IMF
Seletcting appropriate data for train and test phases
OTLBO is used to find out the best parameters of SVM corresponding to minimize the error between observed data and predicted data
Applying test data to classify the status, location and severity of damage of the super tall building
Verification the results by four performance indices including Precision, Recall, Accuracy, and F1_Score

Fig. 1. The flowchart of the suggested model.

2. Equations of motion

Wind loading is the most essential load for super-tall buildings. The following equations describe equations of motion and wind loading of the structures [38]:

$$[M]\{\ddot{X}(t)\} + [C]\{\dot{X}(t)\} + [K]\{X(t)\} = f(t) \quad (1)$$

where M, C, K are mass, damping and stiffness matrixes of the structure with n×n dimension, n is number of degree freedom of structure and f(t) is exciting load (wind load). $\ddot{X}(t)$, $\dot{X}(t)$ and X(t) are acceleration, velocity and displacement vectors of structural responses with n×1 dimension.

Mathematical description of wind load is as follow [39]:

$$u(z,t) = \bar{u}(z) + \bar{u}(z,t) \quad (2)$$

where $\bar{u}(z)$ represents for the mean wind speed and $\bar{u}(z,t)$ for the fluctuating wind speed. Equation (3) can be used to compute the time-varying wind load f(z, t) at the height z m [39].

$$f(z,t) = \frac{1}{2}\rho\mu a_{\omega} u^2(z,t) \quad (3)$$

where ρ signifies air density, μ the aerodynamic force coefficient, and $a_\omega$the orthogonal exposed wind area for the specified section. Equation (3) can be transformed into Equation (4), which decomposes the time-varying wind load into two parts: the average wind load and the fluctuating wind load which the following equations show them [39]:

$$f(z,t) = \bar{f}(z) + \bar{f}(z,t) \tag{4}$$

$$\bar{f}(z) = \frac{1}{2}\rho\mu a_\omega(z)\left[u^2(z) + E[u^2(z,t)]\right] \tag{5}$$

$$\bar{f}(z,t) = \rho\mu a_\omega(z)\bar{u}(z)\bar{u}(z,t) + \frac{1}{2}\rho\mu a_\omega(z)\left[u^2(z) - E[u^2(z,t)]\right] \tag{6}$$

Equation (7) can be used to compute the average wind load in addition to the formula in Equation (5) [39]:

$$\bar{f}(z) = \frac{1}{2}\rho\mu a_\omega(z)[\bar{u}^2(z)] \tag{7}$$

The mean wind speeds at various heights, according to reference [39], follow the power law, and is calculated as follow:

$$\bar{u}(z) = \bar{u}_g\left(\frac{z}{z_g}\right)^\alpha \tag{8}$$

where $\bar{u}_g$ represents the mean wind speed at z_g meters, and z_g stands for the gradient height. α is a constant exponent, ranging approximately between 0.1 and 0.4, based on the terrain's roughness [39].

3. Signal processing methods

As previously discussed, this research utilizes WT for filtering the acceleration response. Following this, MEMD is applied to derive relevant features for identifying structural damages. The following subsections describe the methods.

3.1. Wavelet transform

The WT is utilized to capture the frequency attributes of a signal within a brief time span and to depict the evolution of these attributes over time. It involves the comprehensive conversion of a sequence of elementary functions for various frequency resolutions, yielding frequency components at varying resolutions [40]. Hence, several studies have used the WT [41–44] to monitor the condition of the structures. WT is categorized into two principal types: Continuous Wavelet Transform (CWT) and Discrete Wavelet Transform (DWT). The mathematical description of CWT is as follows [40]:

$$CWT_{s,\tau}^{x(t)\Psi(t)} = \frac{1}{\sqrt{|s|}}\int_{-\infty}^{\infty} x(t)\psi^*\left(\frac{t-\tau}{s}\right)dt \tag{9}$$

Where s and τ are the scale and translation parameters, respectively. ψ^* represents the complex conjugate of the ψ wavelet function. In wavelet analysis, the wavelet function is characterized by

these scale and transition parameters, facilitating non-stationary multi-resolution analysis. Consequently, the WT can select and analyze both small and large intervals within the signal, with small scales focusing on fine details and large scales capturing broader trends. Scales below 1 are associated with signal approximations, whereas scales above 1 relate to the details of the signal.

Mostly, the DWT is used to analyze discrete-time sequences, such as real-valued functions involving time and frequency. It utilizes filter banks to decompose and reconstruct signals, employing wavelet and scaling functions linked to high-pass and low-pass filters. Decomposition filters, represented by pairs of even-length real-valued vectors, split the signal into various resolution bands. These filters are built upon compactly supported orthonormal sequences, each defined accordingly [45]:

$$\Psi_{s,\tau}(n) = \frac{1}{\sqrt{s}}\Psi(\frac{n-b}{s}) \tag{10}$$

In the DWT, the coefficients ($W_{s,b}$) are computed using an inner product, where each coefficient signifies the degree of correlation between the wavelet and a segment of the signal. The wavelet kernel in the DWT is expressed as follows [45]:

$$W_{s,b} = \frac{1}{\sqrt{s}}\sum_{k=+\infty}^{k=-\infty} x(k)\cdot\psi^*(\frac{n-b}{s}) \tag{11}$$

Where $\Psi(\frac{n-b}{s})$ represents the sliding window that facilitates time localization, s denotes the scaling factor, and b denotes the shift factor. When $|s| < 1$, the wavelet support is narrower in time, corresponding to higher frequencies. Conversely, when $|s| > 1$, $\psi_s, b\ (n)$ exhibits a broader time support compared to ψ(n), corresponding to lower frequencies.

Hence, the DWT possesses an orthogonality property and effectively captures characteristics of sequences localized in scaling factor (s) and shift factor (b). Within each frequency band, there are both low and high components, where the low-frequency subset can be further decomposed until reaching the desired resolution. This process involves simultaneously passing the data through low-pass and high-pass filters, each having a specific cutoff frequency (Fs/2), progressively reducing the signal's bandwidth at every level. The procedure starts at the smallest scales and advances towards the largest, with the scale size doubling at each step. This progression can continue up to a selected level, determined by the required resolution, sample size, and sampling rate.

With each scaling of the wavelet function ψ(t) to enhance signal resolution, the wavelet's support is divided by 2, and the average component density is inversely proportional to the dyadic scale 1/2j. Consequently, the number of components is halved after each iteration. As the scaling factor j increases, the wavelet function ψ(t) traverses the signal in time, iteratively refining the decomposition to achieve optimal representation. This iterative process results in multi-resolution analysis .Mathematically, the low-frequency component of the signal x(n) at level j, along with its approximation, can be defined as follows [45]:

$$a_{s,b} = 2^{\frac{-s}{2}}\sum_n x(n)\emptyset(2^{-s}n-b), h_s(n) = \sum_{b=-\infty}^{\infty} a_{s,b}\,\emptyset_{s,b}(n) \tag{12}$$

In this context, φ (n) represents the scaling function, which is analogous to ψ (t) but exclusively comprises positive values. It serves the purpose of smoothing the signal through low-pass filtering, thereby eliminating high-frequency components from the signal. The high-frequency component dj,k at the jth level and the detailed signal gj(n) are subsequently defined as follows [45]:

$$d_{s,b} = \sum_n x(n)\psi_{s,b}(n),\ g_s(n) = \sum_{b=-\infty}^{\infty} d_{s,b}\,\psi_{s,b}(n) \tag{13}$$

The reconstructed signal x(n) can be obtained by utilizing all the high-frequency components at all levels, which are summed together [45].

$$x(n) = \sum_{b=-\infty}^{\infty} a_{s,b}\emptyset_{s,b}(n) + \sum_{s=1}^{s}\sum_{b=-\infty}^{\infty} d_{s,b}\psi_{s,b}(n) \tag{14}$$

Equation (5) suggests that processing the signal to infinite resolutions is impractical. Instead, a more feasible approach involves splitting the signal until the Sth level and then reconstructing it using the approximation at the last level (S) along with all the details [45].

$$x(n) = \sum_{s=-\infty}^{\infty} g_s(n) = \sum_{s=-\infty}^{\infty}\sum_{b=-\infty}^{\infty} d_{s,b}\psi_{s,b}(n) \tag{15}$$

For this study, a suitable frequency range is chosen, with efforts made to minimize noise while filtering out both extremely low and high structural frequencies. This is achieved using a WT that utilizes the Daubechies-5 mother wavelet function. For instance, the wind loading frequency example for structures like the Milad Tower and Canton Tower falls within the range of 0–25 Hz.

3.2. Multivariate EMD

Huang's method for Intrinsic Mode Functions (IMFs) method divides a signal into oscillatory waveforms [17]. A signal has an IMF if it fits the following criteria: (1) In the whole data set, extrema and zero-crossings must be identical or vary by one. (2) The envelopes formed by the local maxima and minima have zero mean values at any place. Sifting is the process of becoming an IMF:

(1) Identify every local extremum in the test data.

(2) Connect all local maxima with a cubic spline upper envelope.

(3) Repeat the technique to create the lower envelope for the local minima. The following describes the first IMF [17,18]:

$$i_1(t) = X(t) - h_1 \tag{16}$$

where $i_1(t)$ is an IMF, X(t) is the original signal, and h_1 is the mean. Using $i_1(t)$ as the initial data, the filtering procedure repeats until the IMF condition is fulfilled. The continuity formula subtracts the signal from the IMF to split the data into a given number of IMFs [17,18]:

$$X(t) = \sum_{j=1}^{n} i_j\,(t) + r_n \tag{17}$$

As mentioned, EMD is capable of processing signals that consist of a single data. It is univariate and mixing mode-prone. MEMD was developed to estimate multi-channel signals [17]. MEMD,

treats n-variate signals as multidimensional time series, generating multidimensional direction vectors. These signals are projected onto direction vectors to assess all multidimensional envelopes. The local mean of signals is determined by averaging all envelopes. To evaluate uniformly distributed groups in MEMD, the Monte Carlo lower deviation sequence creates uniformly distributed point sets on an (n-1)-dimensional sphere [46]. The n-dimensional input $Y(t) = \{y_1(t), y_2(t), \dots y_n(t)\}$ represents the multivariate signal with n components, and $D^k = \{d_1^k, d_2^k, , \dots d_3^k, \}$ represents the direction vectors over the k-th directions on an (n-1)-dimensional sphere. MEMD continues by:

- Choose a directed D-shaped set vector.
- Evaluate the projection of the input signal $Y(t)$ over the k-th direction vector, X_k.
- Determine the time instants, t_i^k, at which the projected signal's maxima, $p^k(t)$, occur for all k.
- To create multivariate envelopes, $\epsilon^k(t)$, interpolate $[t_i^k, Y(t_i^k)]$.
- Use the following equation to determine the mean of the envelope $\bar{m}(t)$ [17]:

$$\bar{m}(t) = \frac{1}{L}\sum_{k=1}^{L} \epsilon^k(t) \tag{18}$$

Assess the residual components $R(t)$, $R(t) = Y(t) - \bar{m}(t)$ evaluates residual components $\epsilon^k(t)$. If it meets the iteration stopping criteria, estimate $Y(t) - R(t)$, and if not, calculate $R(t)$ until it does.

4. Developed hybrid SVM classifier model

The following subsections describe mythology of optimal SVM model using for classification.

4.1. Parameters of support vector machine

SVM utilize linear or nonlinear functions to get the best fit line for classification and damage detection [31,47,48]. SVM is mathematically described as follows [49]:

$$f(x) = W^T \varphi(x) + b \tag{19}$$

where W^T is an m-dimensional weight vector, b represents the bias term, and the mapping function(.) transforms x into an m-dimensional feature vector. f(x) represents the observed (target)-input function (x). Equation specifies an SVM hard margin (primal issue) (12). To solve the equation, the hard margin is converted into a soft margin [49]:

$$Minimize : \frac{1}{2}\|W\|^2 + C\sum_{i=1}^{m}(\xi_i^- + \xi_i^+) \tag{20}$$

$$subject\ to\ \left(w_i.\varphi(x_i) + b_{y_i}\right) - y_i \le \varepsilon + \xi_i^+\ i = 1,2,\dots,m$$

$$y_i - \left(w_i.\varphi(x_i) + b_{y_i}\right) \le \varepsilon + \xi_i^-\ i = 1,2,\dots,m$$

$$\xi_i^-.\xi_i^+ \ge 0 \quad i = 1.2 \dots . m$$

where ξ_i^+ and ξ_i^- are slack variables, W is the vector weight, C is a penalty coefficient, m is the number of inputs, x and y_i are the input and target variables, and ε is an insensitive loss function parameter. The main problem becomes the following equation, which may be utilized to solve equation (13) with restrictions [49]:

$$Minimize: L(w,b,\propto_i^+,\propto_i^-) = \frac{1}{2}\|W\|^2 + C\sum_{i=1}^{m}(\xi_i^- + \xi_i^+) - \sum_{i=1}^{m}\propto_i^+ \left(w_i.\varphi(x_i) + b_{y_i} - y_i + \varepsilon + \xi_i^+\right) - \sum_{i=1}^{m}\propto_i^- \left(y_i - w_i.\varphi(x_i) - b_{y_i} + \varepsilon + \xi_i^-\right) - \sum_{i=1}^{m}(\eta_i\xi_i^+ + \eta_i^*\xi_i^-) \quad (21)$$

where the Lagrange coefficients for the constraints are denoted by $\propto^+$, η_i, $\propto^-$ and η_i^*. Finally, equation (14) is transformed into a dual problem corresponding to the neglect terms of b, w, $\propto^-$ and $\propto^+$ using the Karush-Kuhn-Tucker (KKT) condition and Lagrange function, as shown below [49]:

$$Maximize\ L_D = -\frac{1}{2}\sum_i\sum_j(\alpha_i - \alpha_i^-)\left(\alpha_j - \alpha_j^-\right).k\left(x_i,x_j\right) - \sum_{i=1}^{m}y_i\,(\alpha_i - \alpha_i^-) + \sum_{i=1}^{m}\varepsilon(\alpha_i + \alpha_i^-) \quad (22)$$

$$subject\ to\ \ \sum_{i=1}^{m}(\alpha_i - \alpha_i^-)=0$$

$$k\left(x_i,x_j\right) = \varphi(x_i).\varphi\left(x_j\right) \quad (23)$$

where the kernel function is denoted by $k\left(x_i,x_j\right)$. Thus The Eq. (12) can be expressed as follows [14]:

$$f(x) = \sum_{i=1}^{m}(\alpha_i - \alpha_i^-)\,k\left(x_i,x_j\right) + b \quad (24)$$

In conclusion, the values of the identified parameters, namely, i.e. b, w, α, C and the parameter of the kernel function are used to determine the value of the output. In the current study, the Radial Basis Function (RBF) is used as the kernel function, and its formulation is described as follows [14]:

$$k\left(x_i,x_j\right) = exp\left(\frac{-\|x-x_i\|^2}{2\sigma^2}\right) \quad (25)$$

4.2. Tuned the parameters of support vector machine classifier through OTBLO

OTLBO determines SVM parameters (ε, σ and C) to improve SVM performance. Shahrouzi et al. developed OTLBO, a useful meta-heuristic optimization method [50]. The meta-heuristic algorithm OTLBO enhances TLBO by adding a search mechanism to the teacher phase. It relies on learners communicating random information via memory. The observer is created by randomly selecting the learners' topic-by-topic information. An observer teaches students while the teacher is absent. More search space should improve the algorithm's random search capacity. The OTLBO algorithm, comprising three phases—teacher, observer, and learners—enhances the TLBO algorithm by incorporating both local and global search strategies within the search space, primarily utilizing the observer phase. OTLBO's principal focus lies in [50].

OTLBO must be used to optimize the parameters ε, σ and C of the SVM in order to improve its predictive capability. The processes for creating the SVM-OTLBO classification model are as follow:

- Randomly choosing the starting values of the decision variables ε, σ and C.
- Generating predicted output using SVM based on the training data. The objective function aims to minimize the difference between the predicted output and the observed data.
- The OTLBO method aids in the selection of the optimal SVM parameters by generating new solutions and iteratively updating the best solution based on the objective function.
- Repeating Step (III) satisfies the requirement of the end.

Subsequently, a trained SVM is created, and test data are used to confirm the SVM-OTLBO model's ability to detect the condition of extremely tall structures. The algorithm's flowchart is displayed in Fig. 2. The calculation of the objective function proceeds as follows [30]:

$$Minimize\ Z = 1 - (numel(YPrediction = YTrain)/numel(YTrain)) \quad (26)$$

where $\mathrm{numel}(\mathrm{YPrediction} == \mathrm{YTrain})$ indicates the count of accurately predicted labels, and $\mathrm{numel}(\mathrm{YTrain})$ represents the total count of observed labels.

5. Feature extraction

MEMD has deconstructed IMFs to obtain super-tall building time-domain features. Feature extraction simplifies the complexity of raw data by converting it into a feature vector or another internal representation, thus reducing its dimensionality.

5.1. Time-domain features

Time series data extraction focuses on identifying temporal features. In statistical signal descriptions, the following metrics are utilized: RMS, Variance, Mean, Skewness, Kurtosis, Crest Factor, and Maximum value. Table 1 defines the seven statistical characteristics mathematically.

The procedure of extracting features is as follow:

- WT filters all sensor-collected structural acceleration responses to remove noise and undesired frequencies.
- MEMD splits acceleration responses into IMFs.
- Select the relevant Intrinsic Mode Functions (IMFs) that encompass adequate frequency content of the signals.
- Then, compute statistical time-domain features for each IMF corresponding to each signal (Channel) and compile them into a vector
- Utilize SVM-OTLBO for classification by employing these statistical time-domain vectors.

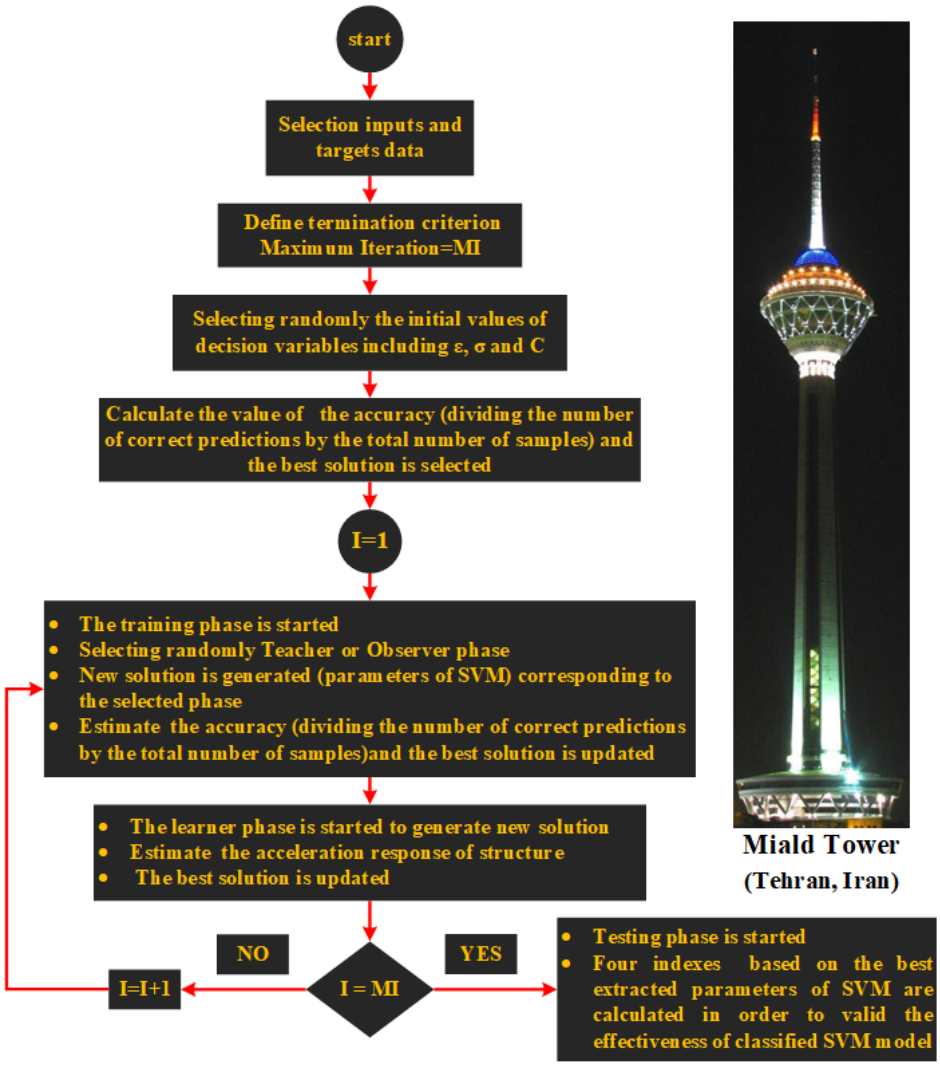
start
Selection inputs and targets data
Define termination criterion Maximum Iteration=MI
Selecting randomly the initial values of decision variables including ε, σ and C
Calculate the value of the accuracy (dividing the number of correct predictions by the total number of samples) and the best solution is selected
I=1
The training phase is started
Selecting randomly Teacher or Observer phase
New solution is generated (parameters of SVM) corresponding to the selected phase
Estimate the accuracy (dividing the number of correct predictions by the total number of samples)and the best solution is updated
The learner phase is started to generate new solution
Estimate the acceleration response of structure
The best solution is updated
NO
YES
I=I+1
I = MI
Testing phase is started
Four indexes based on the best extracted parameters of SVM are calculated in order to valid the effectiveness of classified SVM model
Miald Tower
(Tehran, Iran)

Fig. 2. The flowchart of SVM-OTLBO classified model.

Table 1
Time-domain features.

Feature	Function
Mean	$mean = \frac{\sum_{n=1}^{N} x(n)}{N}$
Root mean square	$RMS = \sqrt{\frac{\sum_{n=1}^{N}(x(n))^2}{N}}$
Variance	$VAR = \sigma^2 = \frac{\sum_{n=1}^{N}(x(n) - mean(x))^2}{(N-1)}$
Skewness	$Skewness = \frac{\sum_{n=1}^{N}(x(n) - mean(x))^3}{(N-1)\sigma^3}$
Kurtosis	$Kurtosis = \frac{\sum_{n=1}^{N}(x(n) - mean(x))^4}{(N-1)\sigma^4}$
Crest factor	$crest = \frac{max(x(n))}{RMS}$
Maximum value	$max = max(\lvert x(n) \rvert)$

6. Evaluating the prediction performance

To assess the performance of the SVM-OTLBO model in identifying damage in super-tall buildings, four indexes are evaluated: accuracy, recall, precision, and F1 Score. [30].

$$Precision_i = \frac{TP_i}{TP_i+FP_i} \tag{27}$$

$$Recall_i = \frac{TP_i}{TP_i+FN_i} \tag{28}$$

$$Accuracy = \frac{TP_i+TN_i}{TP_i+TN_i+FP_i+FN_i} \tag{29}$$

$$F_{1\_}Score = \frac{2*Precision_i*Recall_i}{(Precision_i+Recall_i)} \tag{30}$$

where TP_i represents the count of test samples correctly classified under i^{th} category (Ci), FP_i is the number of test samples incorrectly classified under Ci category, TN_i is the number of test samples correctly classified under other categories, and FN_i is the number of test samples incorrectly classified under other categories.

7. Numerical investigation of the proposed method in case study examples

The efficacy of the proposed method in detecting structural deterioration is demonstrated through the analysis of two exceptionally tall structures: The Milad Tower and the Canton Tower. Table 2 illustrates the frequencies of both towers, derived from experimental and numerically simulated data. These results are consistent with findings from other studies [18,51–53]. Additionally, Table 3 shows the damage ranges at the height of the super tall buildings.

Table 2
The experimental and simulated frequencies of Milad and Conton Towers.

Number of Mode	Frequencies			
	Experimental		Simulated	
	Milad	Canton	Milad	Canton
1	0.158	0.092	0.158	0.11
2	0.354	0.134	0.354	0.16
3	0.422	0.366	0.422	0.346
4	0.539	0.421	0.539	0.36
5	0.647	0.476	0.647	0.399
6	0.785	0.506	0.785	0.461
7	0.854	0.519	0.854	0.484
8	0.968	0.794	0.968	0.738
9	1.167	0.965	1.167	0.902
10	1.248	1.153	1.248	0.99

Table 3
Illustrates the damage ranges at the height of the structure.

Scenario of the damage detection	Tower			
	Milad		Canton	
	Height (m)	Damage range (Percent)	Height (m)	Damage range (Percent)
Condition	82-164	5-10	115-230	5-10
Condition	305-388	5-10	461-577	5-10
Severity	254-266	5	392-409	5
Severity	266-278	10	409-443	10
Severity	278-291	15	426-443	15
Severity	291-305	20	443-460	20
Location	Entire tower is divided into 8 equal parts	5	Entire tower is divided into 8 equal parts	5

7.1. The first case study: Milad tower

Within this investigation, the initial case study revolves around the Milad Tower. The subsequent subsections elaborate on the process of identifying damage within the Milad Tower, encompassing both the determination of its location and the assessment of its severity, employing the proposed methodology.

7.1.1. Presentation of Milad tower

Milad Tower, situated in Tehran, holds a multifaceted role. Its relevance to SHM is accentuated by Tehran's proximity to two fault lines of tectonic plates. Standing tall at 436 meters, it ranks among the world's tallest edifices and accommodates a diverse range of enterprises and dining establishments, alongside housing highly sensitive telecommunications infrastructure. The tower comprises several key components, including its base, transitional section, concrete shaft, top structure, and antenna mast. Notably, the lobby boasts a 28-meter-high transitional structure supported by a circular mat foundation measuring 66 meters in diameter and 3 to 4.5 meters in thickness [9]. The 310-m concrete shaft transmits both lateral and vertical forces into the base. The 12-story steel head structure is 247.5 m to 315 m tall. The last part is installing the 308 to 436-m antenna mast.

7.1.2. Identifying structural deterioration of Milad tower

To estimate structural deterioration of Milad Tower, finite element of the super-tall building is modeled in Abacus software. The structural status of Milad Tower is assessed in three stages: identifying damage, its location, and severity. Initially, the building's condition is evaluated under five cases: undamaged, five percent damage at lower and higher heights, and ten percent damage at lower and upper heights, respectively. Figure 3-a illustrates all cases for Milad Tower. The model undergoes random wind loading ten times to collect the structure's acceleration response

for each case. The wind field parameters include: $\rho = 1.25\ {}^{kg}/_{m^3}$, $\alpha = 0.16$, $Z_g = 247m$, $\bar{u}_g = 31\ \frac{m}{s}$, (for a 10-year return period based on statistical studies), $\mu = 1.26$ for the shaft, 1.42 for the head structure and 1.35 for the antenna mast [54]. Based on real SHM system of Milad Tower, 10 acceleration responses of the finite element model are obtained from selected accelerometers at heights of 28, 96, 180, 240, 276, 280, 302, and 420 m [18]. The acceleration responses are calculated according to equations 1-8. In preprocessing, the reverse WTs reconstruct signals (acceleration responses) according to the specified frequency spectrum. The signals are separated into 8 levels depending on the sampling rate to determine the necessary frequency range and remove noise for Milad Tower. The approximate coefficient of level 8 (A8) and detailed coefficients of levels 1, 2, 3, and 4 (D1, D2, D3, D4) are set to zero. Fig. 4 shows the wavelet tree and coefficients for the super-tall building's frequencies. All cases are preprocessed. Then MEMD decomposes filtered signals.

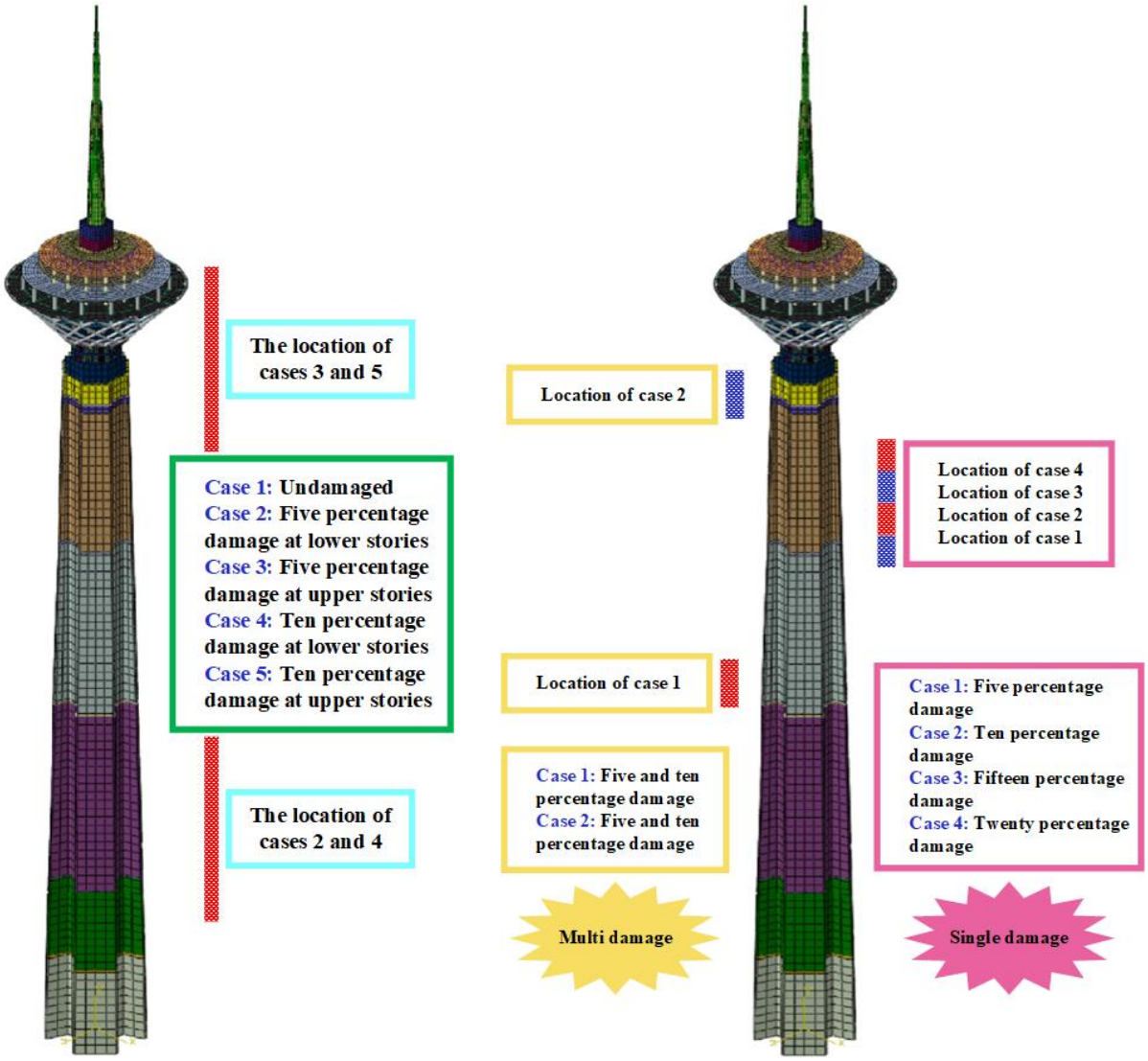
The location of cases 3 and 5
Case 1: Undamaged
Case 2: Five percentage damage at lower stories
Case 3: Five percentage damage at upper stories
Case 4: Ten percentage damage at lower stories
Case 5: Ten percentage damage at upper stories
The location of cases 2 and 4
(a)
Location of case 2
Location of case 1
Case 1: Five and ten percentage damage
Case 2: Five and ten percentage damage
Multi damage
Location of case 4
Location of case 3
Location of case 2
Location of case 1
Case 1: Five percentage damage
Case 2: Ten percentage damage
Case 3: Fifteen percentage damage
Case 4: Twenty percentage damage
Single damage
(b)

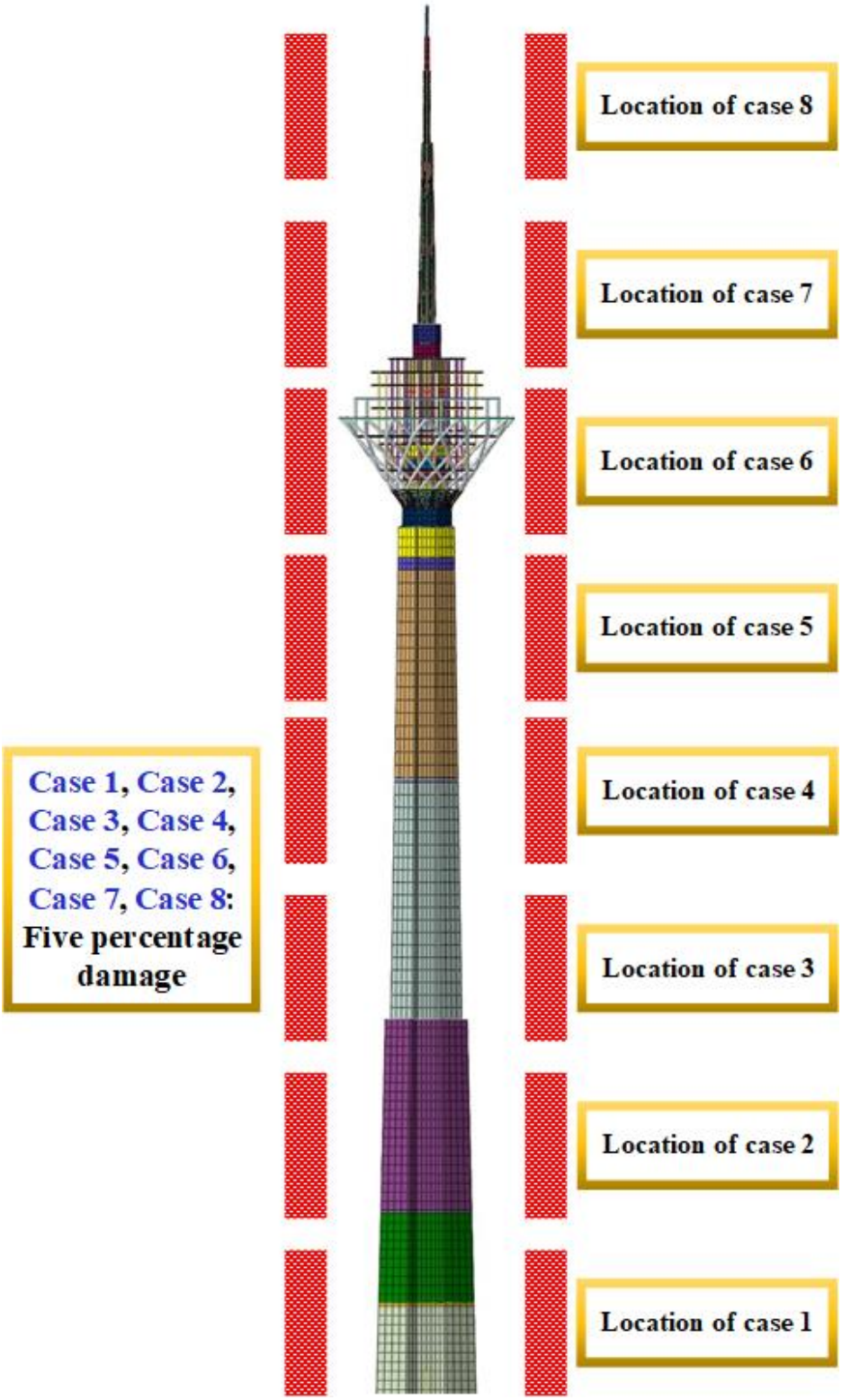
Location of case 8
Location of case 7
Location of case 6
Location of case 5
Location of case 4
Location of case 3
Location of case 2
Location of case 1
Case 1, Case 2, Case 3, Case 4, Case 5, Case 6, Case 7, Case 8: Five percentage damage

(c)

Fig. 3. All cases for identifying the status, location, and severity of damage for Mild Tower (a) is all cases for the status of damage, (b) is all cases for the severity of damage, (c) is all cases for the location of damage.

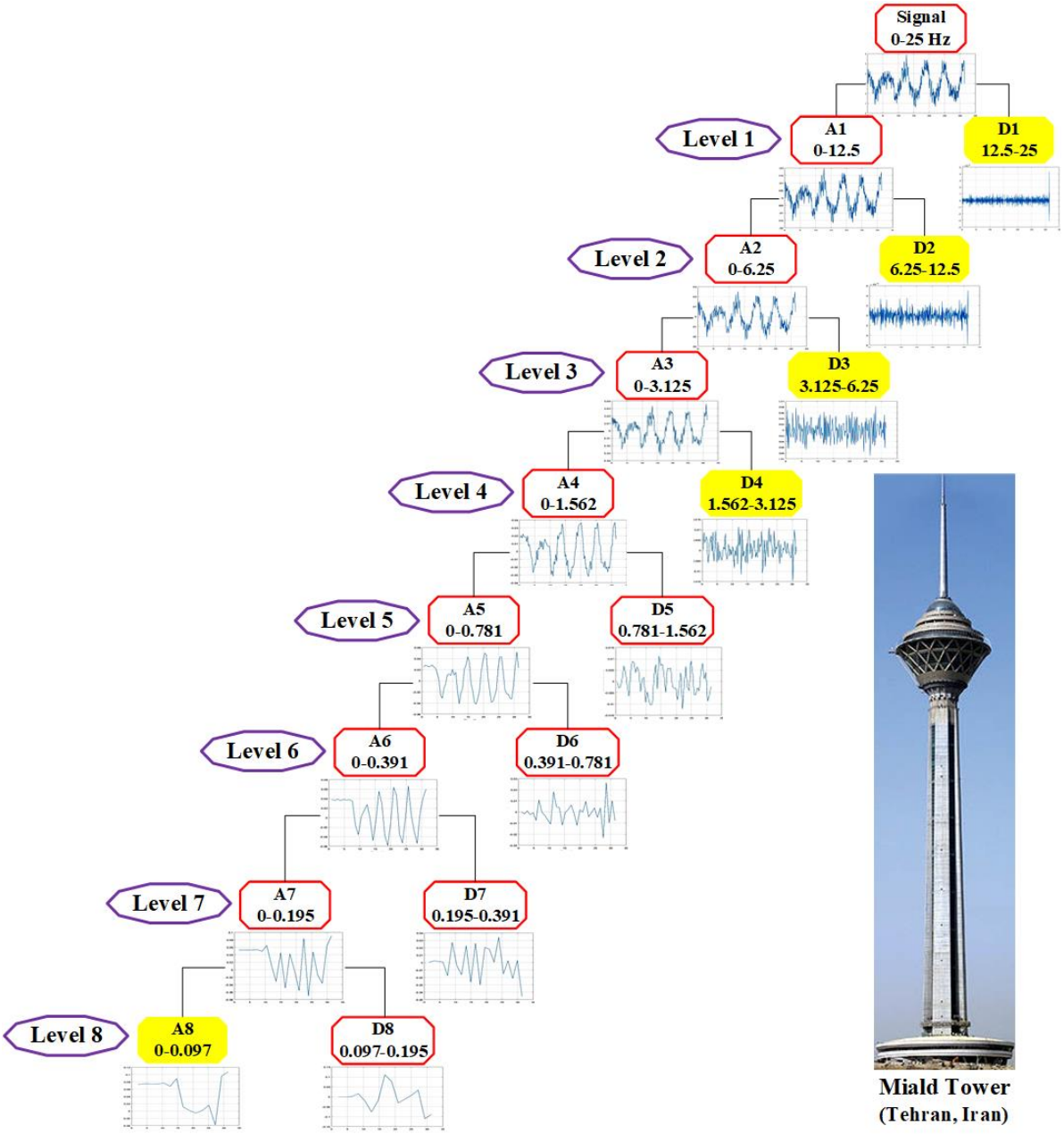

Fig. 4. Wavelet tree, the yellow boxes are omitted detail and approximate coefficients to reconstruct the signals.

Fig. 5 illustrates the Intrinsic Mode Functions (IMFs) of Channel 10. For structural damage detection, five IMFs per channel are selected. Each IMF undergoes extraction of seven statistical features, as outlined in Section 5 and Table 1. Consequently, vectors encompassing all statistical properties of the IMFs for each signal (acceleration response of each channel) are constructed. With each signal segmented into IMFs and five selected, the resulting vector comprises 35 statistical features. 100 samples of data, each with 35 features (5*7 = 35), are generated for each case, resulting in a total of 500 sample data points. Class 1 denotes undamaged instances, whereas class 2 represents damaged cases (cases 2, 3, 4, and 5). To mitigate imbalanced data issues, the final dataset is composed of 40% class 1 and 60% class 2 samples. The final sample

data consists of 250 samples, with 70% allocated for training and 30% for testing. SVM-OTLBO is employed to optimize SVM parameters, effectively training the SVM model by minimizing the disparity between observed and predicted data. Following model training, test data is utilized to validate the trained model. It's worth noting that an alternative optimal SVM-OTLBO approach is employed, which excludes the use of wavelets and MEMD for all data. The same strategy extracts statistical features from raw data (no WT and MEMD) and for comparison the effectiveness of optimization approaches another SMV which their parameters are chosen randomly are used. Fig. 6 displays step-one confusion matrices for both techniques. Without filtering and MEMD, the structure's state is 97.3, yet the suggested model is 100% accurate. Hence, WT filtering and signal decomposition increase SVM-OTLBO model performance. Fig. 6 shows that the proposed model outperforms another optimum SVM for two-class data.

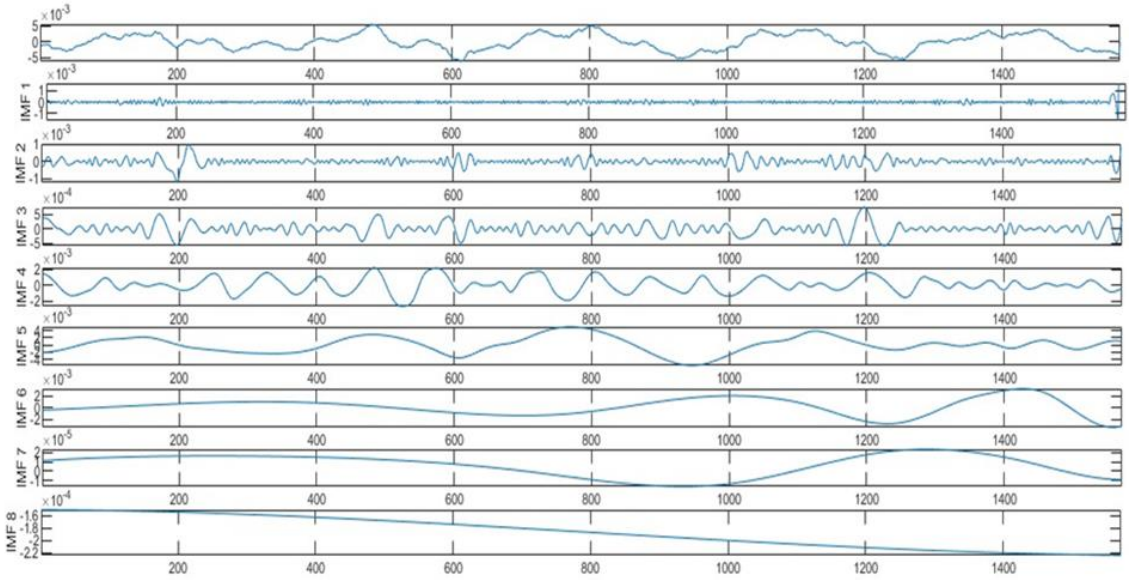

Fig. 5. IMFs of Channel number 10.

(a) (b)

Fig. 6. Confusion matrices of both methods for identifying the statues of Milad Tower that if the tower is damaged or undamaged. (a) Confusion matrices for proposed method, (b) Confusion matrices for second method.

The second phase involves pinpointing the exact location of the damage. The structure is divided into eight parts, and each has 5% damage. Fig. 3-c shows all Milad Tower cases. Hence, there are eight cases like the first step, and the random wind loading is applied 10 times to Milad Tower's finite element model to gather the acceleration response for all cases. The identical process is performed for step two. SVM classifies and recognizes damage location using 800 samples. Damage location is studied by classifying cases 1 to 4 as class one and cases 5 to 8 as class two (first scenario). The second scenario pinpoints damage in a narrower region. The top and lower floors of the structure are investigated. Hence, cases 1 to 2 are class number one, cases 3 to 4 are class number two (Scenario 2 part 1), and the higher level of Millad Tower is studied as follows: cases 5 to 6 are class number one, and cases 7 to 8 are class number two. (Scenario 2, Part 2). The final example involves identifying the location of damage in a smaller region. The damage is examined in four areas. Case 1 is class one, and case 2 is class two (Senario 3 part 1), then case 3 is class number one, and case 4 is class number two (Senario 3 part 2). In the same manner, for the higher cases of structural (Scenario 3 parts 3 and 4), all the states are tested in binary form. As the samples of cases are equal, we do not face unbalanced data, so the sample count across each case remains consistent.

Like step one, 70% of the data is utilized for training and 30% for testing to locate damage. Following the training model, test data are utilized to validate the approach, and another optimum SVM-OTLBO is employed without wavelets and MEMD for all data. Table 4 displays four indices for both damage location techniques. Table 4 shows that the proposed model accurately locates damage in all cases, whereas other SVM-OTLBOs have an accuracy of 91.67 to 100%. Also, for random selecting approach are 88.45 to 95.78%. The suggested technique improves the SVM model's binary classification of damage location in all cases with acceptable accuracy. Hence, WT and MEMD can locate damage. Also, increasing the data accuracy of the proposed method could be better than applying WT and MEMD since the ability of another method is the same as the proposed method for scenario 3, which has less data.

Table 4
Four indexes for deterioration localization of Milad Tower.

	Accuracy			**Recall**			**Precision**			**F_1_Score**		
	Proposed Model	No WT+ MEMD	Random	Proposed Model	No WT+ MEMD	Random	Proposed Model	No WT+ MEMD	Random	Proposed Model	No WT+ MEMD	Random
Scenario 1	100	97.33	92.08	100	97.22	92.12	100	97.22	92.41	100	97.22	92.07
Scenario 2, part 1	100	99.17	91.03	100	99.24	90.82	100	99.09	91.51	100	99.16	91.03
Scenario 2, part 2	100	94.17	94.08	100	94.40	94.22	100	93.91	94.11	100	94.09	94.08
Scenario 3, part 1	100	100	96.16	100	100	96.17	100	100	96.18	100	100	96.32
Scenario 3, part 2	100	100	90.34	100	100	90.61	100	100	90.12	100	100	89.56
Scenario 3, part 3	100	91.67	89.12	100	91.60	90.31	100	91.74	88.45	100	91.65	90.11
Scenario 3, part 4	100	100	95.73	100	100	95.65	100	100	95.67	100	100	95.78

The third step is identifying the severity of the damage. Single damage is assessed first, followed by multiple damages. The single form assumes four damage cases: five percent, ten percent, fifteen percent, and twenty percent. Two cases are considered for multi-damage: case 1 is five percent damage and 10 percent damage at the lower level, and case 2 is the same at the higher level. Fig. 3-b illustrates all Milad Tower cases. There are 400 samples to detected severity of damage. To examine damage severity, case 1 is class number one, while cases 2 to 4 are class number two (scenario 1). All states will be verified in binary form for all structural situations (scenarios 2, 3, and 4). Due to imbalanced data, classes one and two employ 40% and 60% of the samples, respectively. Therefore, the total number of sample data is 220. Also for multi-damage, 200 samples are generated. Like step one, the training and testing stages employ 70% and 30% of the data, respectively, to determine damage severity. Following the training model, test data are utilized to validate the approach, and another optimum SVM-OTLBO is employed without WT or MEMD for all data. The same strategy extracts statistical characteristics from raw data, as indicated. Table 5 displays four damage severity indicators for both approaches. Results show that the suggested technique accurately assesses the damage. All indices, including accuracy, precision, recall, and the F_1_Score, are 95.83–100%, whereas the SVM model without WT and MEMD (the second technique) is 93.33–100%.and for random selecting method are 84.67 to 100%. The suggested classification approach outperforms both other methods in phases one and two (identifying damage and location). Fig. 7 shows the average accuracy, precision, recall, and F_1_Score for Millad Tower septs (damage, position, and severity) and scenarios. Fig. 7 shows that the suggested technique can accurately detect damage status, location, and severity (99.67 to 99.79 percent for all indices), whereas the other method has adequate accuracy (97.58 to 97.63) and for random selection are (92.32 to 92.34).

Table 5
Four indexes for deterioration severity of Milad Tower.

	Accuracy			**Recall**			**Precision**			**F_1_Score**		
	Proposed Model	No WT+ MEMD	Random	Proposed Model	No WT+ MEMD	Random	Proposed Model	No WT+ MEMD	Random	Proposed Model	No WT+ MEMD	Random
Scenario 1	100	97.33	94.17	100	97.22	94.17	100	97.22	93.96	100	97.22	94.23
Scenario 2	100	98.67	91.12	100	98.39	91.12	100	98.89	91.34	100	98.62	90.89
Scenario 3	100	97.33	88.67	100	97.73	87.34	100	96.97	88.33	100	97.27	88.67
Scenario 4	100	100	100	100	100	100	100	100	100	100	100	100
Multi Damage	96.67	93.33	85.33	97.37	93.31	85.13	95.83	93.31	84.67	96.47	93.31	86.33

Fig. 8 illustrates boxplot of all indices for Milad Tower considering all scenarios and cases. The indices in the proposed model are very close to each other and near to 100%, whereas those in other methods are changed between 84 and 100%. According to Fig. 8, the values of the indices of the proposed method are the narrowest and show that the standard division and scattering of them are less than other methods.

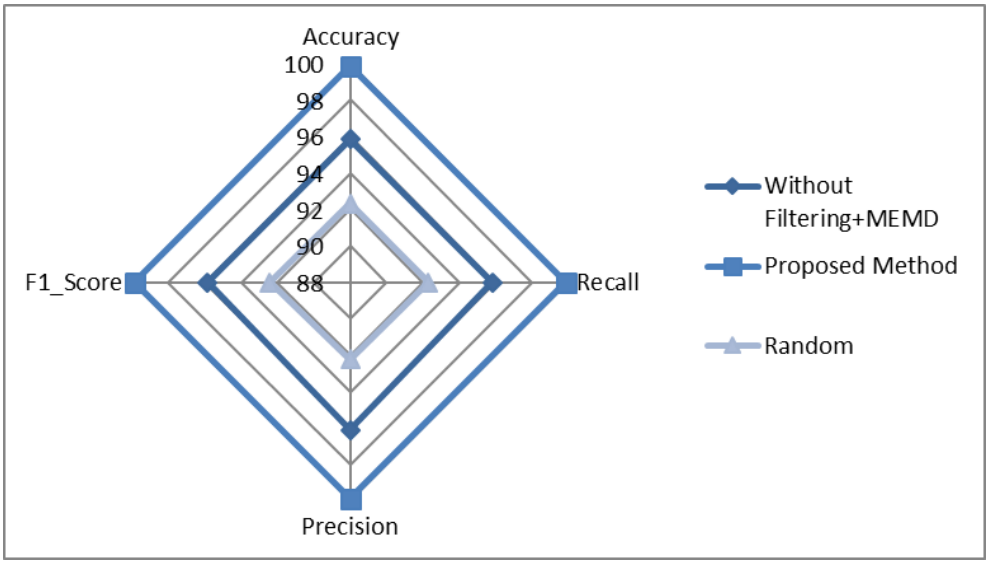

Fig. 7. The average of values of Accuracy, Precision, Recall, and F_1_Score for all septs (damage, location and severity of damage) for all scenarios; Millad Tower.

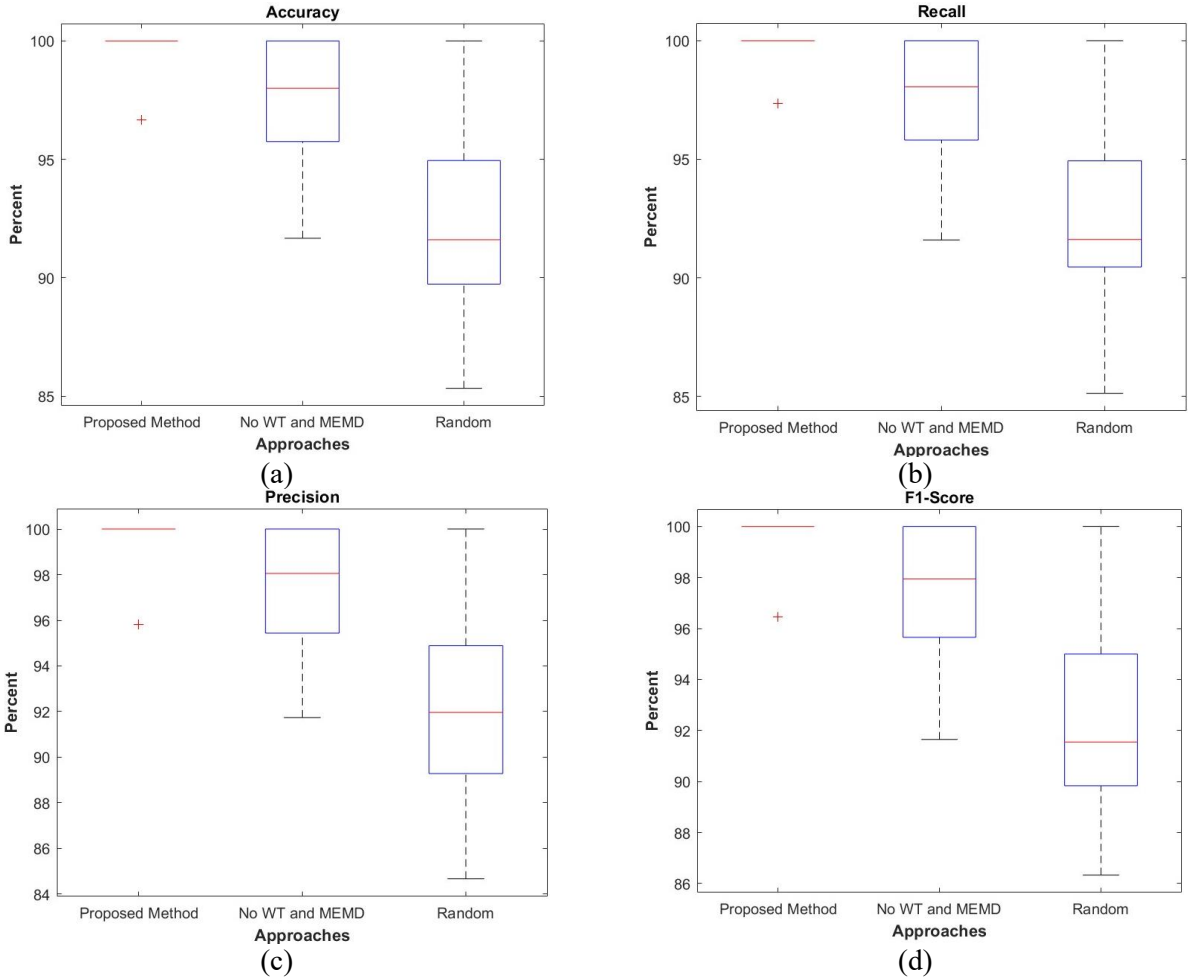

Fig. 8. Boxplot of the values of Accuracy, Precision, Recall, and F_1_Score for all septs (damage, location and severity of damage) for all scenarios; Milad Tower, (a) boxplot for accuracy, (b) boxplot for Precision, (c) boxplot for Recall, (d) boxplot for F_1_Score.

To summarize, based on numerical analyses, the proposed method can identify the condition of structure very well. Not only can the method recognize the status of the structure, but it can also recognize the location and severity of damage with very high precision. One reason for this is that WT can omit noise and set the signals at appropriate frequencies. Also, since the wind excitation signal is non-stationary, the resulting acceleration signals are also non-stationary and nonlinear. Therefore, MEMD is one of the best signal processing methods to deal with this kind of signal (non-stationary and nonlinear signals). Consequently, using WT and MEMD can be an appropriate approach to extracting suitable features to use as inputs for damage detection. Finally, an optimal SVM can recognize a pattern and classify it with properly extracted features. Therefore, the proposed method has an acceptable ability for pattern recognition (classification).

7.2. The second case study: Canton tower

The Canton Tower serves as the second case study in this research, a subject that has attracted considerable scholarly attention. The approach utilized to detect Canton Tower deterioration is described in the following subsections.

7.2.1. Presentation of Canton tower

The other multipurpose building in Guangzhou, China, is the 600 m-tall Canton Tower. A super-tall structure is created from an exterior lattice steel structure connected to an inside reinforced concrete structure by 37 stories at various levels. Canton Tower's structural health must be closely monitored because it is situated on the outskirts of one of the world's most dangerous typhoon zones. The condition of the tower is continuously overseen by an advanced SHM system, equipped with more than 800 sensors. This system diligently records various parameters, including acceleration, wind speed and direction, temperature, and structural deformation, ensuring comprehensive real-time monitoring of the tower's structural integrity and environmental interactions [55,56].

7.2.2. Identifying structural deterioration of Canton tower

Hong Kong Polytechnic University models the super-tall building's finite element to determine Canton Tower's structural deterioration [57]. Like example one, three steps including damage, location, and severity are assumed to assess Canton Tower's structural condition. The same method detects Canton Tower's structural deterioration. First, check whether the building is damaged or undamaged; five instances are considered. Fig. 9-a depicts the locations of all cases on Canton Tower. The wind field has the following parameters $\rho = 1.25\ {}^{kg}/_{m^3}$, $\alpha = 0.22$, $Z_g = 461m$, $\bar{u}_g = 38.7\frac{m}{s}$, (for a 10-year return period based on statistical studies) and more details are in [55]. After calculating the acceleration response (using equations 1–8), WT filters and MEMD decomposes all signals. Time-domain features are retrieved from each signal's five IMFs. Hence, 500 data samples are created, with 40% of the data from case 1 (class 1) and 60% from other instances to avoid imbalance (class 2). Also, the classification of data is similar to that of Milad Tower. The optimal SVM uses 220 sample data points. Similar to Example 1, another

SVM-OTLBO model without using WT and MEMD is applied to damage detection at Canton Tower in order to comparison with the proposed model. Fig. 10 shows the step one confusion matrices for both techniques. Without filtering and MEMD, the structure's state is 93.3%; however, the suggested model is 100% accurate. Hence, WT filtering and signal decomposition increase SVM-OTLBO model performance. Fig. 10 shows that the proposed model outperforms another optimum SVM for two-class data.

The second step deals with the location of the damage. Eight cases are assumed in the entire Canton Tower. Fig. 9-b shows cases. Eight parts of the tower cause 5% damage each. 800 samples have been collected since applying 10-time wind loads. The approach used is similar to Milad Tower, which indicates cases 1–4 are class 1, and cases 5–8 are class 2. And the approach will continue to classify fewer areas like Milad Tower. Hence, seven damage detection scenarios are investigated. Training and testing consume 70% and 30% of the data, respectively. Table 6 shows the results. The suggested model's accuracy to locate damage in all situations is 100%, whereas another SVM-OTLBOs' accuracy is between 90.83 and 100% and for random selecting method are 84.13 to 93.67%. Therefore, the suggested method has sufficient ability to detect the location of the damage.

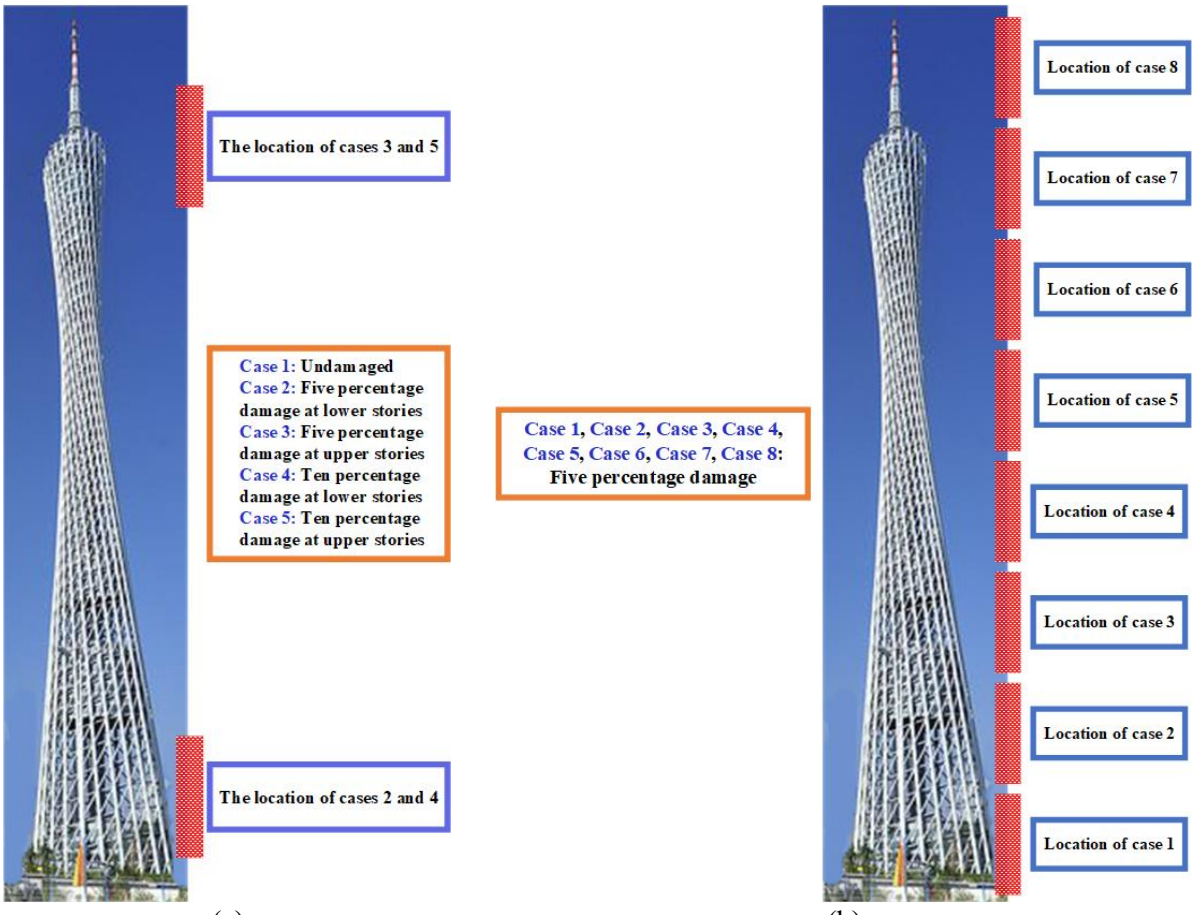
The location of cases 3 and 5
Case 1: Undamaged
Case 2: Five percentage damage at lower stories
Case 3: Five percentage damage at upper stories
Case 4: Ten percentage damage at lower stories
Case 5: Ten percentage damage at upper stories
The location of cases 2 and 4
Case 1, Case 2, Case 3, Case 4, Case 5, Case 6, Case 7, Case 8: Five percentage damage
Location of case 8
Location of case 7
Location of case 6
Location of case 5
Location of case 4
Location of case 3
Location of case 2
Location of case 1

(a) (b)

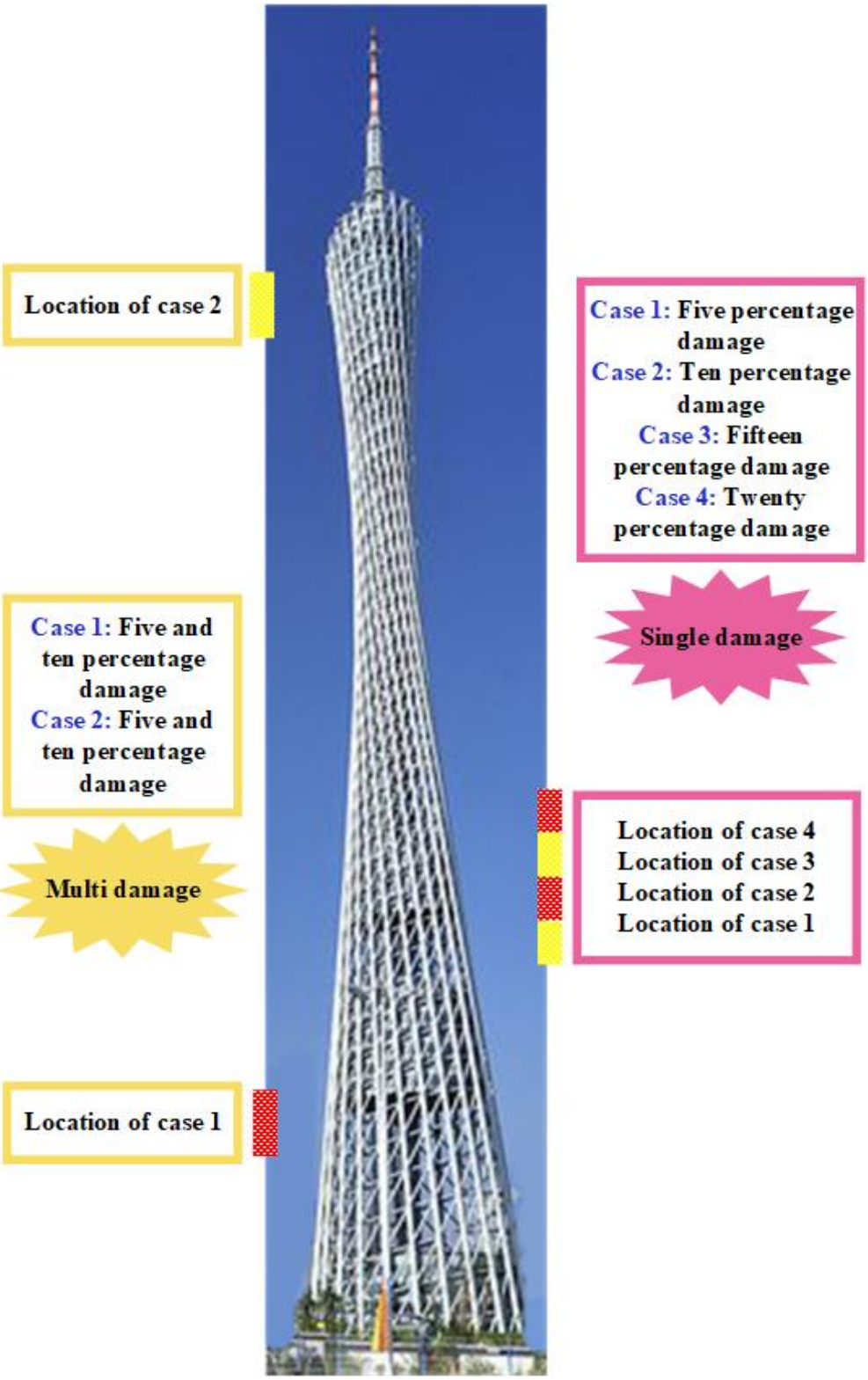
Location of case 2
Case 1: Five percentage damage
Case 2: Ten percentage damage
Case 3: Fifteen percentage damage
Case 4: Twenty percentage damage
Single damage
Case 1: Five and ten percentage damage
Case 2: Five and ten percentage damage
Multi damage
Location of case 4
Location of case 3
Location of case 2
Location of case 1
Location of case 1

(c)

Fig. 9. All cases for identifying the status, location and severity of damage for Canton Tower. (a) Status of damage, (b) Location of damage, (c) Severity of damage.

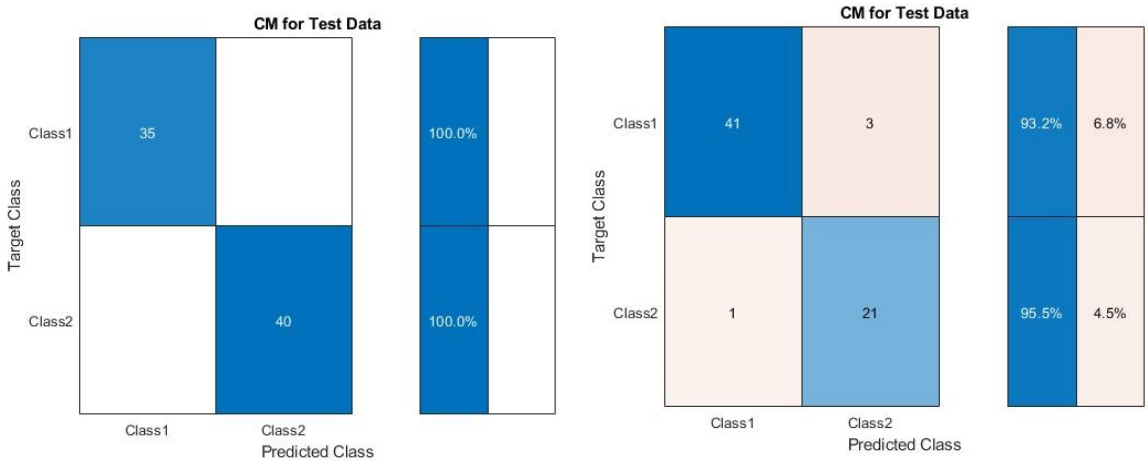

(a) (b)

Fig. 10. 10 Confusion matrices of both methods for identifying the statues of Canton Tower that if the tower is damaged or undamaged. (a) Confusion matrices for proposed method, (b) Confusion matrices second method.

Table 6
Four indexes for deterioration localization of Canton Tower.

	Accuracy			**Recall**			**Precision**			**F_1_Score**		
	Proposed Model	No WT+ MEMD	Random	Proposed Model	No WT+ MEMD	Random	Proposed Model	No WT+ MEMD	Random	Proposed Model	No WT+ MEMD	Random
Scenario 1	100	95.42	91.18	100	95.76	91.22	100	94.95	91.51	100	95.35	91.17
Scenario 2, part 1	100	90.83	92.13	100	90.74	91.72	100	90.84	92.41	100	90.78	92.15
Scenario 2, part 2	100	96.67	93.44	100	96.61	93.55	100	96.92	93.16	100	96.65	93.18
Scenario 3, part 1	100	100	97.22	100	100	97.22	100	100	97.42	100	100	97.48
Scenario 3, part 2	100	93.33	91.24	100	93.75	91.41	100	91.87	91.12	100	92.67	90.48
Scenario 3, part 3	100	98.33	90.21	100	98.15	91.21	100	98.53	89.32	100	98.31	91.21
Scenario 3, part 4	100	98.33	94.65	100	98.15	94.76	100	98.53	94.33	100	98.31	94.33

Step three assesses damage severity. Initially, single damage is assessed, then multi-damage. Four instances are assumed: five percent damage, 10 percent damage, 15 percent damage, and 20 percent damage. Multi-damage assumes two cases: case 1 is five and ten percent damage at lower levels, while case 2 is five and ten percent damage at higher levels. All Canton Tower cases are shown in Fig. 9-c. The first instance is presumed to be class 1, and the others are class 2 (Scenario 1) until all cases are reviewed for damage severity (Scenarios 2, 3, and 4). To minimize the imbalance, 60% of the data is from class 2 and 40% from class 1. Like other steps, SVM-OTLBO is used to compare the results to the suggested method without considering WT and MEMD. Table 7 presents the numerical results for identifying the severity of the damage. The suggested model, like earlier phases, can accurately assess damage severity (98.33 to 100% for

all indices), whereas another way is between 91.32 and 100%. Lastly, Fig. 11 shows the average accuracy, recall, precision, and F_1_Score for all steps (damage, location, and severity) and scenarios for Canton Tower. Fig. 11 shows that the suggested technique can accurately identify damage status, location, and severity (99.87 percentages for all indices), whereas the other method has adequate accuracy (95.86, 95.64, 95.76, and 95.57 for accuracy, recall, precision, and F_1_Score, respectively) and for random selectin are almost 92. Fig. 12 illustrates boxplot of all indices for Canton Tower considering all scenarios and cases. The indices in the proposed model are very close to each other and near to 100%, whereas those in other methods are changed between 84 and 100%. According to Fig. 12, the values of the indices of the proposed method are the narrowest and show that the standard division and scattering of them are less than another method.

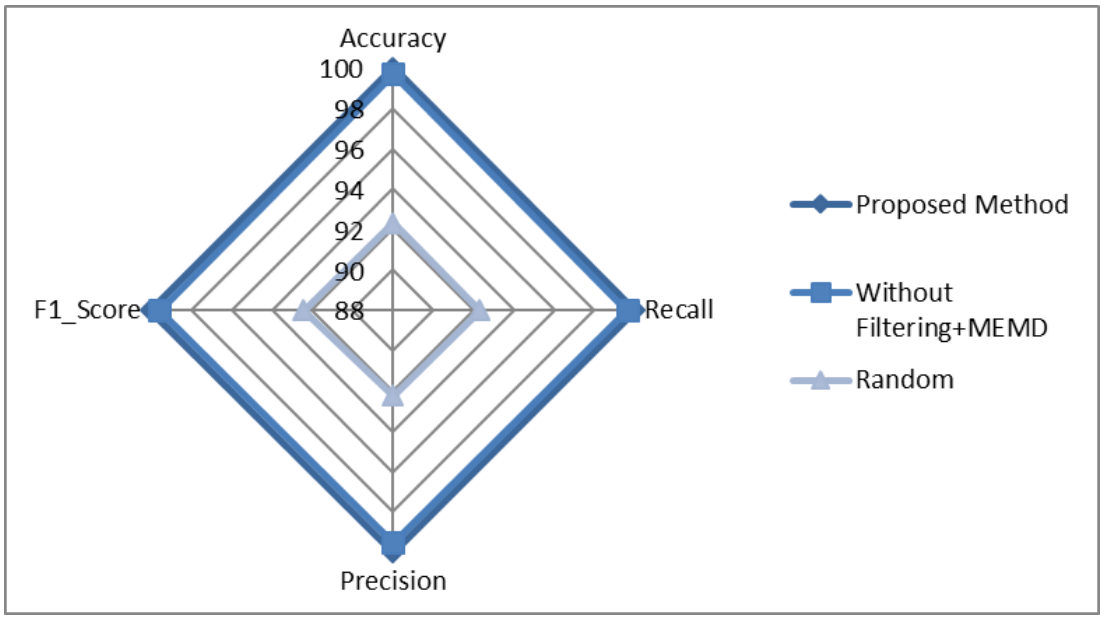

Fig. 11. The average of values of Accuracy, Precision, Recall, and F_1_Score for all septs (damage, location and severity of damage) for all scenarios; Canton Tower.

Table 7
Four indexes for deterioration severity of Canton Tower.

	Accuracy			**Recall**			**Precision**			**F_1_Score**		
	Proposed Model	No WT+ MEMD	Random	Proposed Model	No WT+ MEMD	Random	Proposed Model	No WT+ MEMD	Random	Proposed Model	No WT+ MEMD	Random
Scenario 1	100	97.33	93.33	100	98.08	93.16	100	96	93.67	100	96.93	93.33
Scenario 2	100	96	90.13	100	95.31	90.13	100	96.74	90.67	100	95.86	89.67
Scenario 3	100	92	87.13	100	91.32	87.04	100	91.32	86.57	100	91.32	87.34
Scenario 4	100	97.33	93.24	100	97.31	93.12	100	97.31	93.34	100	97.31	92.88
Multi Damage	98.33	96.67	85.67	98.39	96.67	85.33	98.33	96.87	84.13	98.33	96.66	86.67

Analytical methods may identify structural conditions using the provided strategy. The approach accurately determines the structural condition, damage location, and severity. WT and MEMD can remove noise, adjust appropriate signal frequencies, handle nonlinear and nonstationary signals, and consider all signals simultaneously. Hence, WT and MEMD may be used to extract suitable features for damage detection. Consequently, the optimal SVM can classify the correct extracted features and identify a pattern. The proposed method may recognize patterns in an appropriate manner as a result (classification).

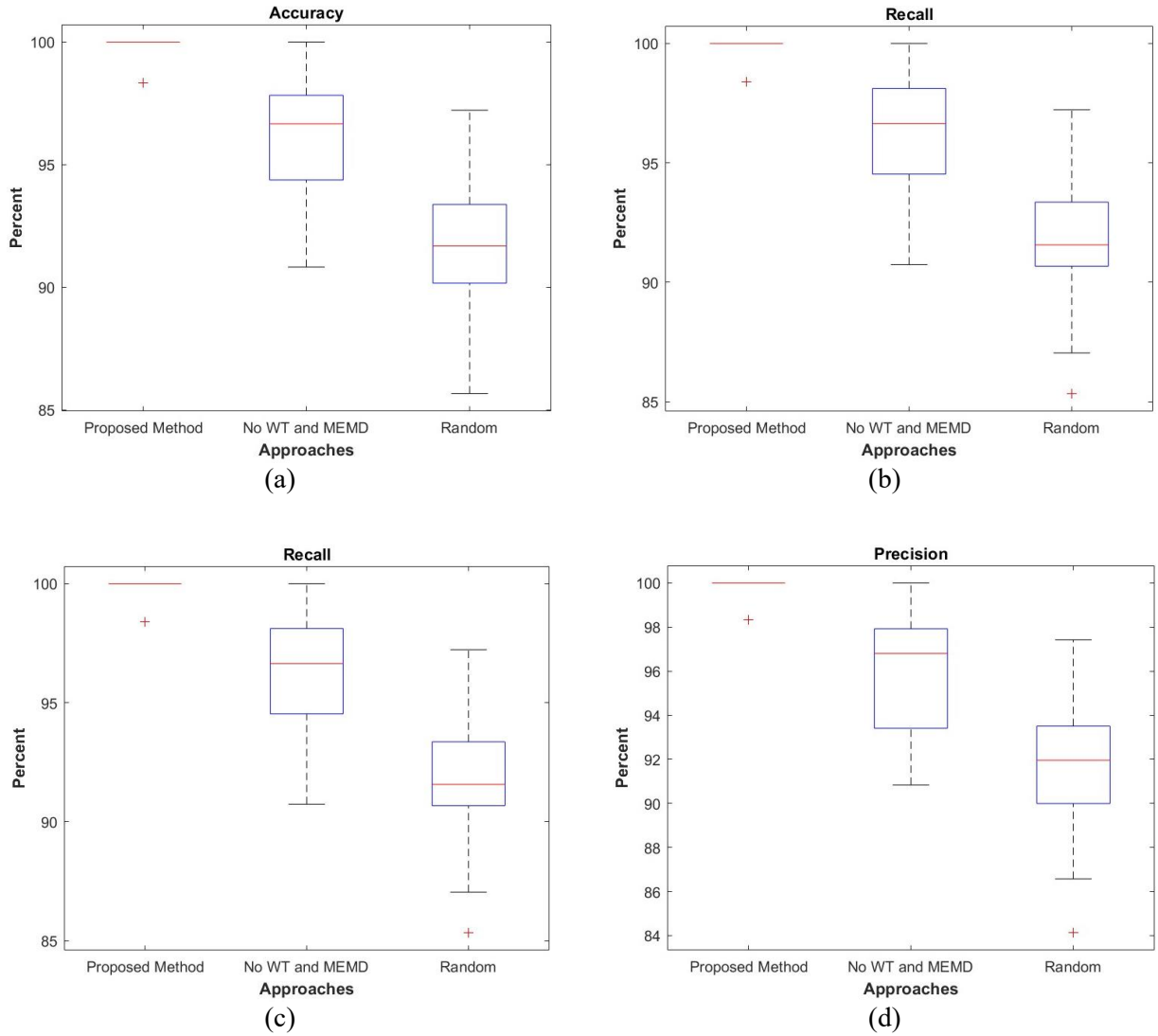

Fig. 12. Boxplot of the values of Accuracy, Precision, Recall, and F_1_Score for all septs (damage, location and severity of damage) for all scenarios; Canton Tower, (a) boxplot for accuracy, (b) boxplot for Precision, (c) boxplot for Recall, (d) boxplot for F_1_Score.

8. Conclusions

This study focused on detecting damage in super-tall buildings, specifically the Milad and Canton Towers, using SVM optimized by OTLBO. Statistical time-domain features were

extracted by integrating signal processing methods such as WT and MEMD. To assess the classification capability of the SVM-OTLBO model, it was compared with another SVM-OTLBO model that did not utilize WT and MEMD, and also did not incorporate optimization techniques. Four indices were employed for evaluation. Based on the obtained numerical results, the following concluding remarks are presented:

- The proposed method exhibited excellent performance in identifying the state, location, and severity of damage within these structures. The accuracy, precision, recall, and F1-Score ranged between 99.7% and 99.8% for both towers, significantly outpacing the alternative method's 95.8% to 97.7% range. This underscores the proposed method's superior reliability and effectiveness in SHM.
- A critical aspect of the pattern recognition process was the feature extraction. While tuning the SVM's unknown parameters could enhance its pattern recognition capabilities, the integration of WT with MEMD proved instrumental in developing an effective approach for extracting time-domain features. These features served as the input for the SVM classification model, demonstrating the method's robustness in damage detection across numerical analyses.
- The accuracy of the proposed model remained consistently high, even with increased data volume. This stability is attributed to the strategic selection of feature extraction methods that gather both time and frequency domain data. The combination between WT and MEMD plays a pivotal role, facilitating a comprehensive feature set conducive to accurate classification.
- By employing MEMD, the proposed methodology was capable of simultaneously processing all necessary data (acceleration response), thereby enhancing the depth of data exploration and establishing a more reliable damage detection system. This multi-dimensional data consideration further strengthens the method's effectiveness in distinguishing structural integrity.

Funding

This research received no external funding.

Conflicts of interest

The authors declare no conflict of interest.

Authors' contributions statement

RD, SHHL: Conceptualization; RD: Data curation; AA: Formal analysis; SHHL, MS: Investigation; RD, SHHL: Methodology; SHHL, MS: Project administration; AA: Resources; RD, AA: Software; SHHL, MS: Supervision; RD: Validation; AA: Visualization; RD, AA: Roles/Writing – original draft; RD, SHHL, MS: Writing – review & editing.

References

[1] Farrar CR, Worden K. An introduction to structural health monitoring. vol. 520. Springer International Publishing; 2010. https://doi.org/10.1007/978-3-7091-0399-9_1.

[2] Balageas D, Fritzen CP, Güemes A. Structural Health Monitoring. Struct Heal Monit 2010:1–495. https://doi.org/10.1002/9780470612071.

[3] Amezquita-Sanchez JP, Adeli H. Signal Processing Techniques for Vibration-Based Health Monitoring of Smart Structures. Arch Comput Methods Eng 2016;1:1–15. https://doi.org/10.1007/S11831-014-9135-7.

[4] Wan HP, Ni YQ. Bayesian multi-task learning methodology for reconstruction of structural health monitoring data: Struct Heal Monit 2018;18:1282–309. https://doi.org/10.1177/1475921718794953.

[5] Chen WH, Lu ZR, Lin W, Chen SH, Ni YQ, Xia Y, et al. Theoretical and experimental modal analysis of the Guangzhou New TV Tower. Eng Struct 2011;33:3628–46. https://doi.org/10.1016/J.ENGSTRUCT.2011.07.028.

[6] Guo YL, Kareem A, Ni YQ, Liao WY. Performance evaluation of Canton Tower under winds based on full-scale data. J Wind Eng Ind Aerodyn 2012;104–106:116–28. https://doi.org/10.1016/J.JWEIA.2012.04.001.

[7] Shi W, Shan J, Lu X. Modal identification of Shanghai World Financial Center both from free and ambient vibration response. Eng Struct 2012;36:14–26. https://doi.org/10.1016/J.ENGSTRUCT.2011.11.025.

[8] Su JZ, Xia Y, Chen L, Zhao X, Zhang QL, Xu YL, et al. Long-term structural performance monitoring system for the Shanghai Tower. J Civ Struct Heal Monit 2013 31 2013;3:49–61. https://doi.org/10.1007/S13349-012-0034-Z.

[9] Yahyai M, Rezayibana B, Daryan AS. Nonlinear seismic response of Milad Tower using finite element model. Struct Des Tall Spec Build 2009;18:877–90. https://doi.org/10.1002/TAL.468.

[10] Zhang Q, Yang B, Liu T, Li H, Lv J. Structural Health Monitoring of Shanghai Tower Considering Time-dependent Effects. Int J High-Rise Build 2015;4:39–44. https://doi.org/10.21022/IJHRB.2015.4.1.039.

[11] Wan H-P, Ni Y-Q. Bayesian Modeling Approach for Forecast of Structural Stress Response Using Structural Health Monitoring Data. J Struct Eng 2018;144:04018130. https://doi.org/10.1061/(ASCE)ST.1943-541X.0002085.

[12] Wu J, Xu H, Zhang Q. Dynamic performance evaluation of Shanghai Tower under winds based on full-scale data. Struct Des Tall Spec Build 2019;28:e1611. https://doi.org/10.1002/tal.1611.

[13] Wang Y-W, Ni Y-Q. Full-scale monitoring of wind effects on a supertall structure during six tropical cyclones. J Build Eng 2022;45:103507. https://doi.org/10.1016/J.JOBE.2021.103507.

[14] Doroudi R, Lavassani SHH, Shahrouzi M. Predicting acceleration response of super-tall buildings by support vector regression. Struct Des Tall Spec Build 2023;32:e2049. https://doi.org/10.1002/TAL.2049.

[15] Sadhu A. An integrated multivariate empirical mode decomposition method towards modal identification of structures: J Vib Control 2015;23:2727–41. https://doi.org/10.1177/1077546315621207.

[16] Babajanian Bisheh H, Ghodrati Amiri G, Nekooei M, Darvishan E. Damage detection of a cable-stayed bridge based on combining effective intrinsic mode functions of empirical mode

decomposition using the feature selection technique. Inverse Probl Sci Eng 2021;29:861–81. https://doi.org/10.1080/17415977.2020.1814280.

[17] Rehman NU, Park C, Huang NE, Mandic DP. EMD via MEMD: multivariate noise-aided computation of standard EMD. Adv Adapt Data Anal 2013;05:1350007. https://doi.org/10.1142/S1793536913500076.

[18] Doroudi R, Lavassani SHH, Shahrouzi M, Dadgostar M. Identifying the dynamic characteristics of super tall buildings by multivariate empirical mode decomposition. Struct Control Heal Monit 2022;29:e3075. https://doi.org/10.1002/STC.3075.

[19] Ghiasi R, Ghasemi MR, Chan THT. Optimum feature selection for SHM of benchmark structures using efficient AI mechanism. Smart Struct Syst 2021;27:623–40. https://doi.org/10.12989/SSS.2021.27.4.623.

[20] Avci O, Abdeljaber O, Kiranyaz S, Hussein M, Gabbouj M, Inman DJ. A review of vibration-based damage detection in civil structures: From traditional methods to Machine Learning and Deep Learning applications. Mech Syst Signal Process 2021;147:107077. https://doi.org/10.1016/J.YMSSP.2020.107077.

[21] Nayak SC, Nayak SK, Panda SK. Assessing compressive strength of concrete with extreme learning machine. J Soft Comput Civ Eng 2021;5:68–85. https://doi.org/10.22115/SCCE.2021.286525.1320.

[22] Zhang C, Mousavi AA, Masri SF, Gholipour G, Yan K, Li X. Vibration feature extraction using signal processing techniques for structural health monitoring: A review. Mech Syst Signal Process 2022;177:109175. https://doi.org/10.1016/J.YMSSP.2022.109175.

[23] Nouri Y. Structural Damage Detection in the Wooden Bridge Using the Fourier Decomposition , Time Series Modeling and Machine Learning Methods. J Soft Comput Civ Eng 2024;8:83–101. https://doi.org/10.22115/scce.2023.401971.1669.

[24] Dadrasajirlou Y, Ghazvinian H, Heddam S, Ganji M. Reference Evapotranspiration Estimation using ANN, LSSVM, and M5 Tree Models (Case Study: of Babolsar and Ramsar Regions, Iran). J Soft Comput Civ Eng 2022;6:103–21. https://doi.org/10.22115/scce.2022.342290.1434.

[25] Meharie MG, Shaik N. Predicting highway construction costs: Comparison of the performance of random forest, neural network and support vector machine models. J Soft Comput Civ Eng 2020;4:103–12. https://doi.org/10.22115/SCCE.2020.226883.1205.

[26] Ghazvineh S, Nouri G, Hosseini Lavasani SH, Gharehbaghi V, Noroozinejad Farsangi E, Noori M. 7 Vibration-based damage detection using a novel hybrid CNN-SVM approach. Data-Centric Struct Heal Monit 2023:137–58. https://doi.org/10.1515/9783110791426-007.

[27] Chong JW, Kim Y, Chon KH. Nonlinear multiclass support vector machine–based health monitoring system for buildings employing magnetorheological dampers: J Intell Mater Syst Struct 2013;25:1456–68. https://doi.org/10.1177/1045389X13507343.

[28] Nguyen TH, Vu AT. Comparison of machine learning classifiers for reducing fitness evaluations of structural optimization. J Soft Comput Civ Eng 2021;5:57–73. https://doi.org/10.22115/SCCE.2021.306249.1367.

[29] Sun L, Shang Z, Xia Y, Bhowmick S, Nagarajaiah S. Review of Bridge Structural Health Monitoring Aided by Big Data and Artificial Intelligence: From Condition Assessment to Damage Detection. J Struct Eng 2020;146:04020073. https://doi.org/10.1061/(ASCE)ST.1943-541X.0002535.

[30] Doroudi R, Hossein S, Lavassani H. Optimal tuning of three deep learning methods with signal processing and anomaly detection for multi-class damage detection of a large-scale bridge. Struct Heal Monit 2024. https://doi.org/10.1177/14759217231216694.

[31] Doroudi S, Sharafati A, Mohajeri SH. Satellite-based estimation of daily suspended sediment load using hybrid intelligent models. Hydrol Sci J 2023;68:1–18. https://doi.org/10.1080/02626667.2022.2156292.

[32] Afshar A, Nouri G, Ghazvineh S, Hosseini Lavassani SH. Machine-Learning Applications in Structural Response Prediction: A Review. Pract Period Struct Des Constr 2024;29. https://doi.org/10.1061/PPSCFX.SCENG-1292.

[33] Kaveh A, Bakhshpoori T. Metaheuristics: Outlines, MATLAB Codes and Examples. Springer International Publishing; 2019. https://doi.org/10.1007/978-3-030-04067-3/COVER.

[34] Shahrouzi M, Kaveh A. An efficient derivative-free optimization algorithm inspired by avian life-saving manoeuvres. J Comput Sci 2022;57:101483. https://doi.org/10.1016/j.jocs.2021.101483.

[35] Takin K, Doroudi R, Doroudi S. Vibration control of structure by optimising the placement of semi-active dampers and fuzzy logic controllers. Aust J Struct Eng 2021;22:1–14. https://doi.org/10.1080/13287982.2021.1957198.

[36] Lavasani SHH, Doroudi R. Meta heuristic active and semi-active control systems of high-rise building. Int J Struct Eng 2020;10:232–53. https://doi.org/10.1504/IJSTRUCTE.2020.108529.

[37] Hosseini Lavassani SH, Mousavi Gavgani SA, Doroudi R. Optimal control of jacket platforms vibrations under the simultaneous effect of waves and earthquakes considering fluid-structure interaction. Ocean Eng 2023;280:114593. https://doi.org/10.1016/j.oceaneng.2023.114593.

[38] Doroudi R, Lavasani SHH. Connection of coupled buildings: A state-of-the-art review. Structures 2021;33:1299–326. https://doi.org/10.1016/J.ISTRUC.2021.05.017.

[39] Simiu E, Yeo D. Wind Effects on Structures. Chichester, UK: John Wiley & Sons, Ltd; 2019. https://doi.org/10.1002/9781119375890.

[40] Khanahmadi M, Gholhaki M, Rezaifar O, Dezhkam B. Signal processing methodology for detection and localization of damages in columns under the effect of axial load. Meas J Int Meas Confed 2023;211:112595. https://doi.org/10.1016/j.measurement.2023.112595.

[41] Khanahmadi M, Mirzaei B, Amiri GG, Gholhaki M, Rezaifar O. Vibration-based damage localization in 3D sandwich panels using an irregularity detection index (IDI) based on signal processing. Measurement 2024;224:113902. https://doi.org/10.1016/j.measurement.2023.113902.

[42] Naderpour H, Fakharian P. A synthesis of peak picking method and wavelet packet transform for structural modal identification. KSCE J Civ Eng 2016;20:2859–67. https://doi.org/10.1007/s12205-016-0523-4.

[43] Dadgostar M, Setarehdan SK, Akin A. Detection of motion artifacts in fNIRS via the continuous wavelet transform. 2013 20th Iran Conf Biomed Eng ICBME 2013 2013:243–6. https://doi.org/10.1109/ICBME.2013.6782227.

[44] Fakharian P, Naderpour H. Damage Severity Quantification Using Wavelet Packet Transform and Peak Picking Method. Pract Period Struct Des Constr 2022;27:1–11. https://doi.org/10.1061/(ASCE)SC.1943-5576.0000639.

[45] Silik A, Noori M, Altabey WA, Ghiasi R. Selecting optimum levels of wavelet multi-resolution analysis for time-varying signals in structural health monitoring. Struct Control Heal Monit 2021;28. https://doi.org/10.1002/stc.2762.

[46] Barbosh M, Sadhu A, Vogrig M. Multisensor-based hybrid empirical mode decomposition method towards system identification of structures. Struct Control Heal Monit 2018;25:e2147. https://doi.org/10.1002/STC.2147.

[47] Gui G, Pan H, Lin Z, Li Y, Yuan Z. Data-driven support vector machine with optimization techniques for structural health monitoring and damage detection. KSCE J Civ Eng 2017 212 2017;21:523–34. https://doi.org/10.1007/S12205-017-1518-5.

[48] Pan H, Azimi M, Gui G, Yan F, Lin Z. Vibration-based support vector machine for structural health monitoring. Lect. Notes Civ. Eng., vol. 5, Springer; 2018, p. 167–78. https://doi.org/10.1007/978-3-319-67443-8_14.

[49] Doroudi S, Sharafati A, Mohajeri SH. Estimation of Daily Suspended Sediment Load Using a Novel Hybrid Support Vector Regression Model Incorporated with Observer-Teacher-Learner-Based Optimization Method. Complexity 2021;2021:13. https://doi.org/10.1155/2021/5540284.

[50] Shahrouzi M, Aghabagloua M, Rafiee F. Observer-teacher-learner-based optimization: An enhanced meta-heuristic for structural sizing design. Struct Eng Mech 2017;62:537–50. https://doi.org/10.12989/sem.2017.62.5.537.

[51] Zhang FL, Ni YQ, Ni YC, Wang YW. Operational modal analysis of Canton Tower by a fast frequency domain Bayesian method. Smart Struct Syst 2016;17:209–30. https://doi.org/10.12989/SSS.2016.17.2.209.

[52] Niu Y, Kraemer P, Fritzen CP. Operational modal analysis for Canton Tower. Smart Struct Syst 2012;10:393–410. https://doi.org/10.12989/SSS.2012.10.4_5.393.

[53] Kuok SC, Yuen KV. Structural health monitoring of Canton Tower using Bayesian framework. Smart Struct Syst 2012;10:375–91. https://doi.org/10.12989/SSS.2012.10.4_5.375.

[54] Ghorbani-Tanha AK, Noorzad A, Rahimian M. Mitigation of wind-induced motion of Milad Tower by tuned mass damper. Struct Des Tall Spec Build 2009;18:371–85. https://doi.org/10.1002/tal.421.

[55] Niu Y, Fritzen CP, Jung H, Buethe I, Ni YQ, Wang YW. Online Simultaneous Reconstruction of Wind Load and Structural Responses—Theory and Application to Canton Tower. Comput Civ Infrastruct Eng 2015;30:666–81. https://doi.org/10.1111/MICE.12134.

[56] Yi TH, Li HN, Zhang XD. Health monitoring sensor placement optimization for Canton Tower using immune monkey algorithm. Struct Control Heal Monit 2015;22:123–38. https://doi.org/10.1002/STC.1664.

[57] Ni YQ, Xia Y, Liao WY, Ko JM. Technology innovation in developing the structural health monitoring system for Guangzhou New TV Tower. Struct Control Heal Monit 2009;16:73–98. https://doi.org/10.1002/stc.303.